

**Supporting Information**

**Ligand tuned catalytic activity of Ruthenium-imidazolyl amine complexes  
for reversible formic acid dehydrogenation and CO<sub>2</sub> hydrogenation to  
formic acid**

**Khanindra Kalita, Sanjeev Kushwaha and Sanjay K. Singh\***

Catalysis Group, Department of Chemistry, Indian Institute of Technology Indore, Khandwa Road, Simrol, Indore 453552, Madhya Pradesh, India

E-mail: [sksingh@iiti.ac.in](mailto:sksingh@iiti.ac.in)

Table of content

Description	Page no.
General procedure for calculation of TON and TOF in FA dehydrogenation	S5
<b>Table S1</b> Catalytic FA dehydrogenation in water over <i>in situ</i> <b>Ru/Ln</b> catalysts	S6
<b>Fig. S1</b> GC-TCD analysis of the (a) evolved gas ( $H_2:CO_2 \approx 1:1$ ) for the catalytic FA dehydrogenation over <i>in situ</i> <b>Ru/L7</b> catalyst (Analysis is performed using Argon as the carrier gas). Reaction conditions: FA (0.4 M, 2.5 mL in water), SF (0.25 mmol), <i>in situ</i> <b>Ru/L7</b> catalyst ( <b>Ru</b> : 10 $\mu$ mol, <b>L7</b> : 20 $\mu$ mol) at 90 °C. (b) Pure mixture of gas containing $H_2$ , CO, $CH_4$ , $CO_2$ .	S7
<b>Fig. S2</b> Cyclic voltammograms for (a) <b>Ru</b> (b) <b>Ru/L3</b> (c) <b>Ru/L6</b> (d) <b>Ru/L7</b> (e) <b>Ru/L8</b> and (f) <b>Ru/L9</b> catalysts in acetonitrile with 0.1 M $NBu_4PF_6$ as supporting electrolyte at a scan rate of 0.1 $Vs^{-1}$ .	S8
<b>Table S2.</b> Electrochemical data extracted from cyclic voltammograms of <b>Ru</b> , <b>Ru/L3</b> , <b>Ru/L6</b> , <b>Ru/L7</b> , <b>Ru/L8</b> and <b>Ru/L9</b> complexes	S9
<b>Table S3</b> Kinetics parameters for FA dehydrogenation over <b>Ru/L7</b> catalyst in water.	S10
<b>Fig. S3</b> (a) Temperature dependent FA dehydrogenation over <i>in situ</i> <b>Ru/L7</b> catalyst and (b) the corresponding Arrhenius plot was based on the initial rate at 3 min for FA dehydrogenation. Reaction conditions: FA (0.4 M, 2.5 mL in water), SF (0.25 mmol), <i>in situ</i> <b>Ru/L7</b> catalyst ( <b>Ru</b> : 10 $\mu$ mol, <b>L7</b> : 20 $\mu$ mol), 50°C – 90 °C.	S11
<b>Table S4</b> Activation energies ( $E_a$ ) for FA dehydrogenation in water over various literature known catalysts	S12
<b>Table S5.</b> Determination of activation parameters for FA dehydrogenation over <b>Ru/L7</b> catalyst in water	S13
<b>Fig. S4</b> Eyring plot for FA dehydrogenation. Reaction conditions: FA (0.4 M, 2.5 mL in water), SF (0.25 mmol), <i>in situ</i> <b>Ru/L7</b> catalyst ( <b>Ru</b> : 10 $\mu$ mol, <b>L7</b> : 20 $\mu$ mol), 50°C – 90 °C, where e. u. is the energy unit for $\frac{\Delta S^\ddagger}{R}$ value.	S14
<b>Fig. S5</b> Recyclability plot for catalytic FA dehydrogenation over <i>in situ</i> <b>Ru/L7</b> catalyst. Reaction conditions: FA (0.4 M, 25 mL in water), SF (2.5 mmol), <i>in situ</i> <b>Ru/L7</b> catalyst ( <b>Ru</b> : 10 $\mu$ mol, <b>L7</b> : 20 $\mu$ mol) at 90°C. FA (380 $\mu$ L) was added after each catalytic run. GC-TCD analysis after 80 catalytic runs (inset).	S15

<b>Fig. S6</b> Minor Ru/(Ln) <sub>2</sub> species observed after 70 catalytic runs for FA dehydrogenation over <b>Ru/L7</b> catalyst.	S16
<b>Table S6</b> Upscaling the catalytic FA dehydrogenation over <i>in situ</i> <b>Ru/L7</b> catalyst	S17
<b>Fig. S7</b> Gas evolution plot for upscaling the catalytic FA dehydrogenation over <i>in situ</i> <b>Ru/L7</b> catalyst ( <b>Ru</b> : 10 $\mu\text{mol}$ , <b>L7</b> : 20 $\mu\text{mol}$ ) at 90°C. Reaction conditions: 10 fold: FA (0.4 M, 25 mL in water), SF (2.5 mmol); 20 fold: FA (0.4 M, 50 mL in water), SF (5 mmol); 30 fold: FA (0.4 M, 75 mL in water), SF (7.5 mmol); and 50 fold: FA (0.4 M, 125 mL in water), SF (12.5 mmol).	S18
<b>Fig. S8</b> Long-term stability of the catalytic FA dehydrogenation over <i>in situ</i> <b>Ru/L7</b> catalyst in water at 90 °C, FA (380 $\mu\text{L}$ ) was added after days 15, 36 and 60 days in the same reaction mixture. Reaction conditions: FA (0.4 M, 25 mL in water), SF (2.5 mmol), <b>Ru/L7</b> catalyst ( <b>Ru</b> : 10 $\mu\text{mol}$ , <b>L7</b> : 20 $\mu\text{mol}$ ) at 90°C.	S19
<b>Fig. S9</b> <sup>1</sup> H NMR of reaction aliquot of the catalytic FA dehydrogenation over <i>in situ</i> <b>Ru/L7</b> catalyst in a high pressure reactor (Closed system) GC-TCD analysis of the evolved gas (inset) Reaction conditions: FA (0.4 M, 25 mL in water), SF (2.5 mmol), <i>in situ</i> <b>Ru/L7</b> catalyst ( <b>Ru</b> : 10 $\mu\text{mol}$ , <b>L7</b> : 20 $\mu\text{mol}$ ), at 90 °C.	S20
<b>Fig. S10</b> Control Hg(0) poisoning experiment, with and without a large excess of elemental Hg(0). Reaction conditions: FA (0.4 M, 2.5 mL in water), <i>in situ</i> <b>Ru/L7</b> catalyst ( <b>Ru</b> : 10 $\mu\text{mol}$ , <b>L7</b> : 20 $\mu\text{mol}$ ), SF (0.25 mmol), 90 °C.	S21
<b>Fig. S11</b> Mass analysis of various species formed during the <i>in situ</i> generation of <b>Ru/L7</b> catalyst. Reaction conditions: <b>Ru</b> (10 $\mu\text{mol}$ ), <b>L7</b> (20 $\mu\text{mol}$ ), H <sub>2</sub> O (2.5 mL), 90 °C, 1.5 h.	S22
<b>Fig. S12</b> Formation Ru-formato species <b>Ru/L7-B</b> . (a) Reaction conditions: <b>Ru</b> (10 $\mu\text{mol}$ ), <b>L7</b> (20 $\mu\text{mol}$ ), FA (1 mmol), H <sub>2</sub> O (2.5 mL), 90 °C, 15 min. (b) Reaction conditions: <b>Ru</b> (10 $\mu\text{mol}$ ), <b>L7</b> (20 $\mu\text{mol}$ ), FA (1 mmol), SF (0.25 mmol), H <sub>2</sub> O (2.5 mL), 90 °C, 2 min. Where <b>Ru</b> : $[(\eta^6\text{-C}_{10}\text{H}_{14})\text{RuCl}_2]_2$ .	S23
<b>Fig. S13</b> (a) Mass analysis of Ru hydrido species <b>Ru/L7-C</b> . (b) Temperature dependent <sup>1</sup> H NMR analysis in D <sub>2</sub> O. Reaction conditions: <b>Ru</b> (10 $\mu\text{mol}$ ), <b>L7</b> (20 $\mu\text{mol}$ ), SF (1 mmol), D <sub>2</sub> O (2.5 mL), at 40, 50, 70, 90 °C for 10 min each.	S24
<b>Fig. S14</b> Mass investigation of the reaction mixture of <i>in situ</i> <b>Ru</b> (10 $\mu\text{mol}$ ), <b>L7</b> (20 $\mu\text{mol}$ ), treated with SF (1 mmol) in water (2.5 mL) stirred at 90 °C for 10 min in step 1, and further with 1 M HCl (1 mL) in the step 2.	S25
<b>Table S7</b> Single crystal X-ray refinement data for <b>Ru/L7</b>	S26

<b>Table S8</b> Selected bond lengths (Å) for <b>Ru/L7</b>	S27
<b>Table S9</b> Selected bond angles (°) for <b>Ru/L7</b>	S28-S30
<b>Fig. S15</b> UV-vis spectra of (a) aqueous solution of <b>Ru/L7</b> (black line), (b) aqueous solution of <b>Ru/L7</b> with the addition of SF (red line), and (c) after adding aqueous HCl to an aqueous solution of <b>Ru/L7</b> with the addition of SF (blue line).	S31
<b>Fig. S16</b> UV-vis spectra of aqueous solution of <b>Ru/Ln</b> upon the addition of SF.	S32
<b>Fig. S17</b> Ru-hydride formation rate based on the change in absorption at 400 nm for <b>Ru/Ln</b> complexes in the presence of SF.	S33
<b>Table S10</b> Ru-hydride formation rates for <b>Ru/Ln</b> catalysts in the presence of SF	S34
<b>Fig. S18</b> CO <sub>2</sub> capture and hydrogenation. <b>Dehydrogenation</b> of FA, Reaction conditions: Reaction conditions: FA (0.4 M, 25 mL in water), SF (2.5 mmol), <i>in situ</i> <b>Ru/L7</b> catalyst ( <b>Ru</b> : 10 μmol, <b>L7</b> : 20 μmol) at 90 °C. <b>CO<sub>2</sub> captured</b> (a) <sup>13</sup> C NMR of CO <sub>2</sub> captured reaction aliquot (5 mL of 2 M KOH), GC TCD analysis of effluent gas (inset). <b>Hydrogenation</b> of bicarbonate, Reaction conditions: <i>in situ</i> <b>Ru/L7</b> catalyst ( <b>Ru</b> : 10 μmol, <b>L7</b> : 20 μmol), H <sub>2</sub> (20 bar), 80 °C, 48 h. (b) <sup>1</sup> H (inset) and <sup>13</sup> C NMR (in D <sub>2</sub> O) of reutilization of captured CO <sub>2</sub> reaction aliquot (hydrogenation of HCO <sub>3</sub> <sup>-</sup> )	S35
<b>Fig. S19</b> <sup>1</sup> H NMR spectrum (in DMSO-d <sub>6</sub> ) for generation of Ru-hydrido species and Ru-formato species involved in CO <sub>2</sub> hydrogenation. Reaction conditions: (a) <b>Ru/L7</b> (0.02 mmol) in DMSO (1.5 mL). (b) <i>ex situ</i> <b>Ru/L7</b> (0.02 mmol) in DMSO (1.5 mL), H <sub>2</sub> (20 bar), 80 °C, 2.5 h. (c) <i>ex situ</i> <b>Ru/L7</b> (0.02 mmol) in DMSO (1.5 mL), H <sub>2</sub> (10 bar), CO <sub>2</sub> (10 bar), 80 °C, 2.5 h.	S36
General Procedure for the Synthesis of Ligands ( <b>L2 -L9</b> )	S37-S39
Characterization of ligand <b>L2-L9</b> and metal complex ( <b>Ru/L7</b> )	S40-S54
<b>Table S11</b> Comparative catalytic activity of previous literature work and the current work for formic acid dehydrogenation.	S55-S56
References	S57-S58

### **General procedure for TON and TOF calculation in FA dehydrogenation.**

The turnover number (TON) was calculated by the following equation:

$$\text{TON} = \frac{V_{\text{corrected}}}{\left( V_{m,\text{H}_2, 25^\circ\text{C}} + V_{m,\text{CO}_2, 25^\circ\text{C}} \right) \times n_{\text{catalyst}}} = \frac{\text{Substrate}}{\text{Catalyst}} \times \frac{\text{Conversion (\%)} 100}{100}$$

where,  $V_{\text{measured}}$  and  $V_{\text{blank}}$  are the volume of gas measured in the catalytic reaction and blank reaction,  $V_{\text{corrected}} = V_{\text{measured}} - V_{\text{blank}}$ ,  $V_m$  are the molar volume of  $\text{H}_2$  and  $\text{CO}_2$ , respectively, and  $n_{\text{catalyst}}$  is the molar amount of catalyst. To account for temperature changes that can affect the measurements of evolved gas volume, a blank reaction without any catalyst was performed. The blank volume ( $V_{\text{blank}}$ ) was observed to be constant over the course of the reaction and was used to correct all the measured gas volumes ( $V_{\text{measured}}$ ) generated during FA dehydrogenation. The turnover frequency (TOF) was calculated by the following equation:

$$\text{TOF} = \frac{\text{TON}}{\text{Time}}$$

where time is in hour.

For example, for entry 12 (Table 1) the dehydrogenation of an aqueous solution of FA (1 mmol, 0.4 M in water) with SF (0.25 mmol) at 90 °C, over *in situ* **Ru/L7** catalyst (**Ru**: 10 μmol, **L7**: 20 μmol), in the first 3 min 49 mL gas was released with complete conversion of FA. Therefore, the TON and TOF for this reaction can be calculated as follows:

$$\text{TON} = \frac{1 \text{ mmol}}{0.01 \text{ mmol}} \times \frac{49 \text{ mL}}{49 \text{ mL}} = 100$$

$$\text{TOF} = \frac{100}{3 \text{ min}} \times 60 \text{ min} = 2000 \text{ h}^{-1}$$

**Table S1** Catalytic FA dehydrogenation in water over *in-situ* **Ru/Ln** catalysts

Entry	Catalysts	Volume of gas (mL)	Time (min)	TON	TOF (h <sup>-1</sup> )
1	<b>Ru</b>	35	390	71	193
2	<b>Ru/L1</b>	28	244	57	122
3	<b>Ru/L2</b>	26	167	53	131
4	<b>Ru/L3</b>	38	187	78	196
5	<b>Ru/L4</b>	34	176	69	81
6	<b>Ru/L5</b>	30	127	61	131
7	<b>Ru/L6</b>	49	27	100	322
8	<b>Ru/L7</b>	49	12	100	587
9	<b>Ru/L8</b>	49	19	100	322
10	<b>Ru/L9</b>	46	15	95	261

Reaction condition: FA (0.4 M, 2.5 mL in water), *in situ* **Ru/Ln** catalysts (**Ru**: 10  $\mu$ mol, **Ln**: 20  $\mu$ mol) at 90 °C. TON and TOF values were estimated, respectively at the end of the reaction and initial 3 min. Ru:  $[(\eta^6\text{-C}_{10}\text{H}_{14})\text{RuCl}_2]_2$  and Ln: **L1-L9**.

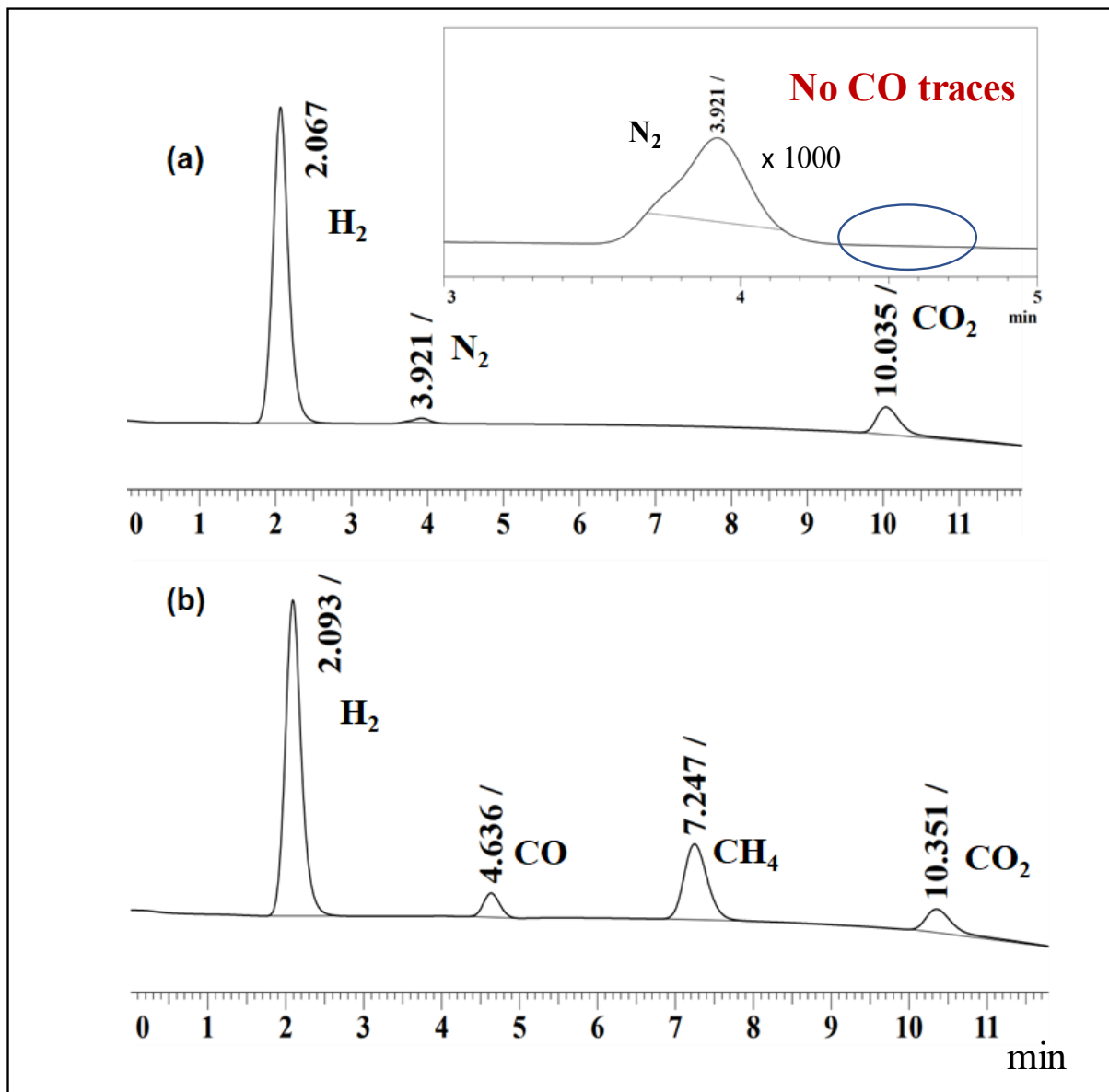


**Fig. S1** GC-TCD analysis of the (a) evolved gas ( $\text{H}_2:\text{CO}_2 \approx 1:1$ ) for the catalytic FA dehydrogenation over *in situ* **Ru/L7** catalyst (Analysis is performed using Argon as the carrier gas). No CO traces (inset). Reaction conditions: FA (0.4 M, 2.5 mL in water), SF (0.25 mmol), *in situ* **Ru/L7** catalyst (**Ru**: 10  $\mu\text{mol}$ , **L7**: 20  $\mu\text{mol}$ ) at 90 °C. (b) Pure mixture of gas containing  $\text{H}_2$ , CO,  $\text{CH}_4$ ,  $\text{CO}_2$ .

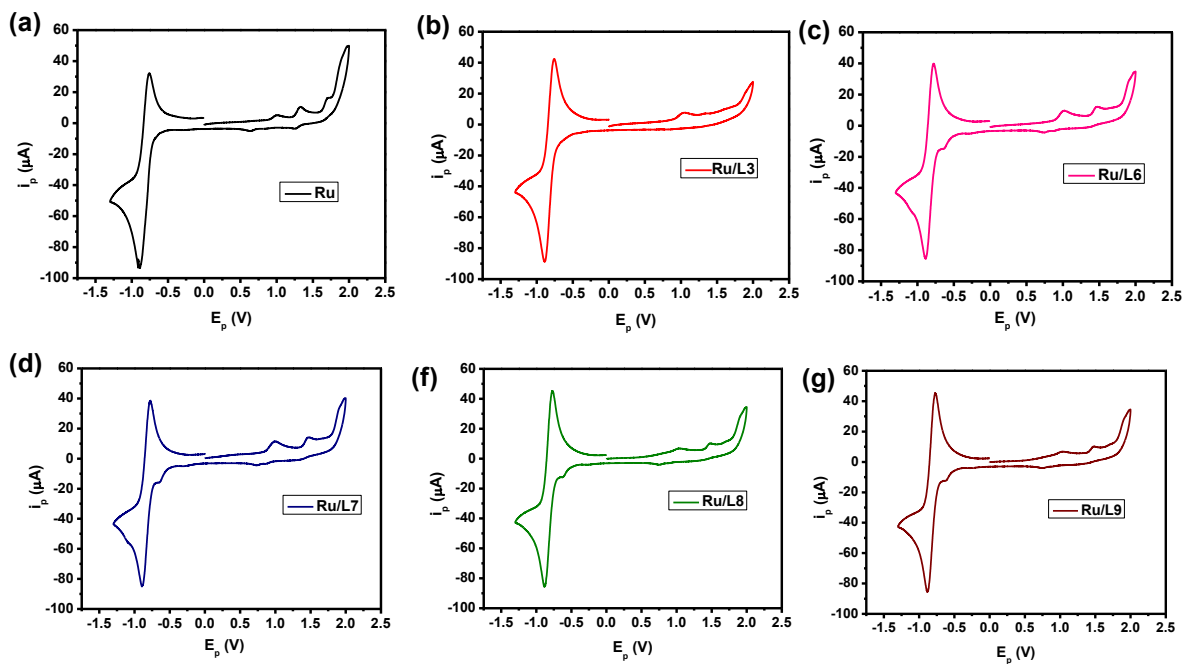


**Fig. S2** Cyclic voltammograms for catalysts (1mM) (a) **Ru** (b) **Ru/L3** (c) **Ru/L6** (d) **Ru/L7** (e) **Ru/L8** and (f) **Ru/L9** in acetonitrile with 0.1 M NBu<sub>4</sub>PF<sub>6</sub> as supporting electrolyte at a scan rate of 0.1 Vs<sup>-1</sup>.

**Table S2** Electrochemical data extracted from cyclic voltammograms of **Ru**, **Ru/L3**, **Ru/L6**, **Ru/L7**, **Ru/L8** and **Ru/L9** complexes

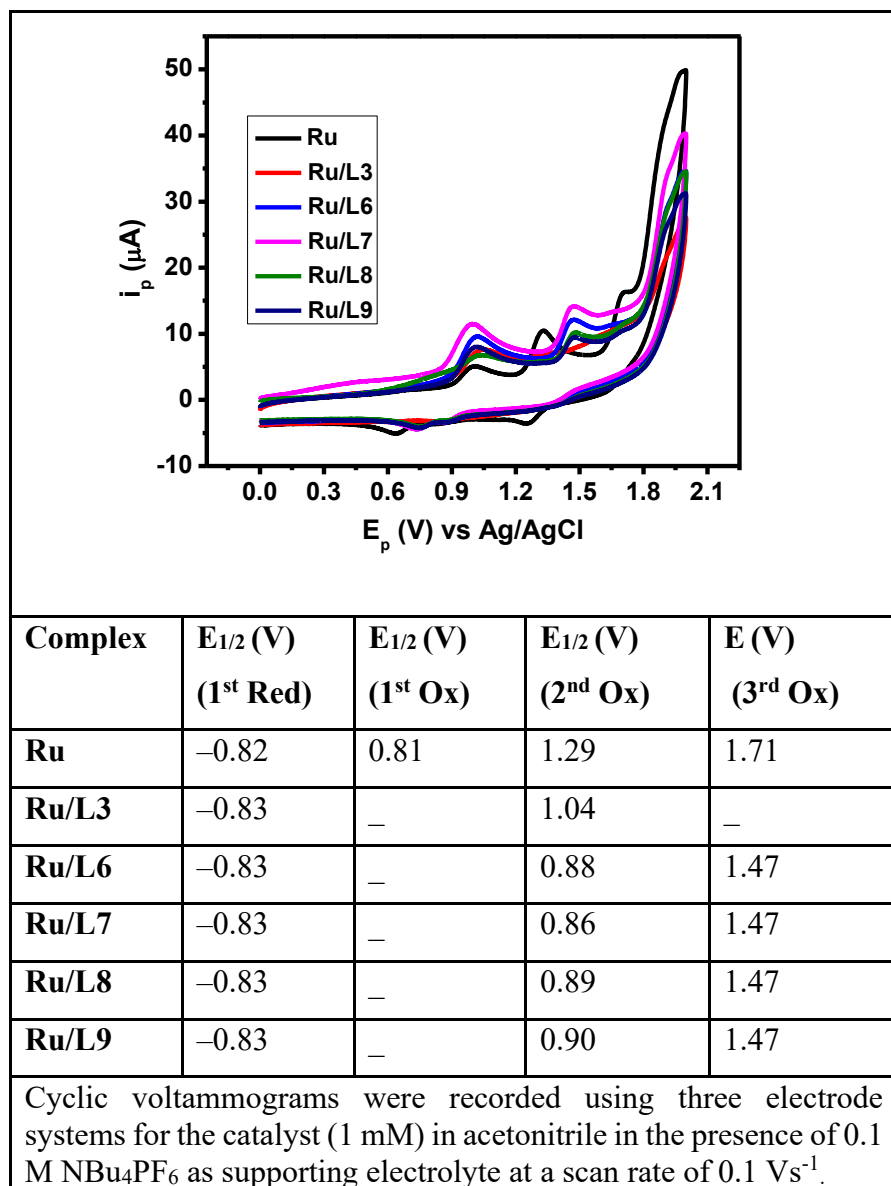


**Table S3** Kinetics parameter for FA dehydrogenation over **Ru/L7** in water

Temperature (K)	$1/T \times 10^3 (K^{-1})$	$k (s^{-1})$	$\ln[k] (s^{-1})$
363	2.75	0.555556	-0.58779
353	2.83	0.253889	-1.37086
343	2.91	0.108889	-2.21743
333	3.00	0.054167	-2.91569
323	3.09	0.022778	-3.78197

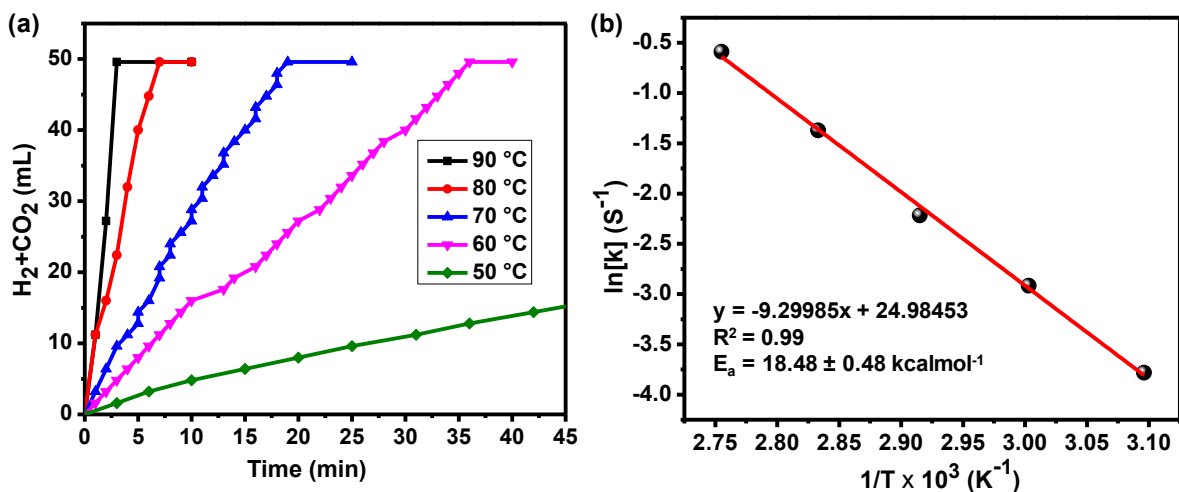


**Fig. S3** (a) Temperature dependent FA dehydrogenation over *in situ* Ru/L7 catalyst and (b) the corresponding Arrhenius plot was based on the initial rate at 3 min for FA dehydrogenation. Reaction conditions: FA (0.4 M, 2.5 mL in water), SF (0.25 mmol), *in situ* Ru/L7 catalyst (**Ru**: 10  $\mu\text{mol}$ , **L7**: 20  $\mu\text{mol}$ ), 50°C – 90 °C.

#### Estimation of activation energy ( $E_a$ ) using Arrhenius plot:

We know the Arrhenius equation as  $k = Ae^{-E_a/RT}$

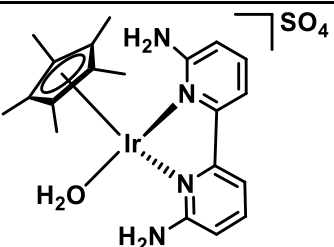
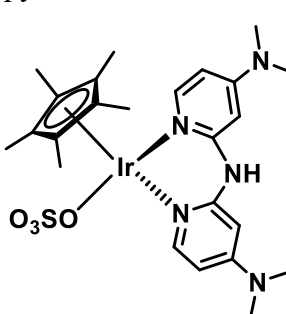
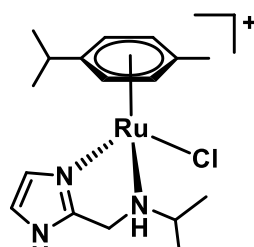
$\ln k = \ln A + (-E_a/R)1/T$ , where  $E_a$  is the activation energy and  $R$  is molar gas constant (1.987 cal K $^{-1}$  mol $^{-1}$ ) and  $T$  is temperature in Kelvin (323 K – 363 K)

From the Arrhenius plot (**Fig. S3**): Slope =  $-9.29985 \pm 0.23939$

As from  $\ln[k]$  vs.  $1/T$  plot, we got slope =  $-E_a / R = -9.29985 \pm 0.23939$

Therefore,  $E_a = 18.48 \pm 0.48 \text{ k cal mol}^{-1}$

**Table S4** Activation energies ( $E_a$ ) for FA dehydrogenation in water over various literature known catalysts

Catalysts	Reaction conditions	$E_a$ (kcalmol <sup>-1</sup> )	Ref.
	HCOOH (1 mol/L M, 2.5 mL), H <sub>2</sub> O, 50-80 °C, 10 min	19.45	S1
[Cp*Ir(pyrimidylimidazoline)H <sub>2</sub> O] SO <sub>4</sub>	HCOOH (1 M, 10 mL), H <sub>2</sub> O, 45-70 °C, 0.17 h	18.69	S2
[Cp*Ir(THBPM)(H <sub>2</sub> O)]SO <sub>4</sub> where THBPM: 2,2',6,6'-tetrahydroxyl-4,4'-bipyrimidine	1 M HCOOH/HCOONa (1:1, 10 mL), H <sub>2</sub> O, 50-80 °C, 0.08 h	18.26	S3
	HCOOH (4 mmol), H <sub>2</sub> O (1.3 mL), 60-90 °C, 5 min	18.49	S4
	HCOOH (0.4 M, 2.5 mL), HCOONa (0.25 mmol), H <sub>2</sub> O, 50-90 °C, 3 min	18.48	This work

**Table S5.** Determination of activation parameters for FA dehydrogenation over **Ru/L7** catalyst in water

T (K)	(1/T) x 10 <sup>3</sup> (K <sup>-1</sup> )	k (s <sup>-1</sup> )	k/T (s <sup>-1</sup> K <sup>-1</sup> )	[k/T x c], where c = h/k', (h = Planck's constant and k' = Boltzmann's constant)	ln[k/T x c] (e. u.)
363	2.75	0.555556	0.00153	7.3309 x 10 <sup>-14</sup>	-30.2441
353	2.83	0.253889	0.000719	3.4451 x 10 <sup>-14</sup>	-30.9992
343	2.91	0.108889	0.000317	1.5206 x 10 <sup>-14</sup>	-31.8171
333	3.00	0.054167	0.000163	7.7916 x 10 <sup>-15</sup>	-32.4857
323	3.09	0.022778	0.0000705	3.3779 x 10 <sup>-15</sup>	-33.3215

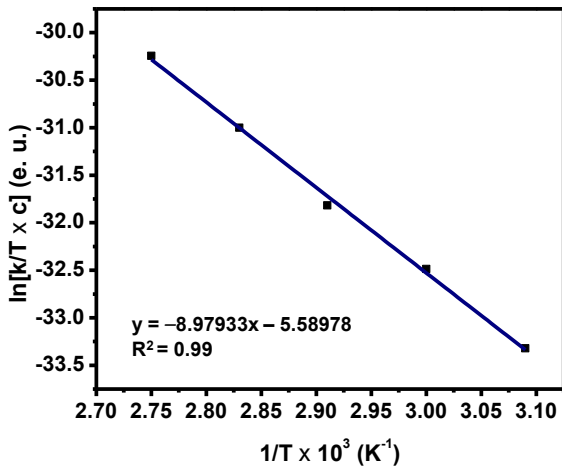


**Fig. S4** Eyring plot for FA dehydrogenation. Reaction conditions: FA (0.4 M, 2.5 mL in water), SF (0.25 mmol), *in situ* **Ru/L7** catalyst (**Ru**: 10  $\mu$ mol, **L7**: 20  $\mu$ mol), 50°C – 90 °C, where e. u. is the energy unit for  $\frac{\Delta S^\ddagger}{R}$  value.

#### Estimation of activation parameters using Eyring plot:

We know the Eyring equation as  $k = \frac{k' T}{h} e^{-\frac{\Delta H^\ddagger}{RT}} e^{\frac{\Delta S^\ddagger}{R}}$

$$\text{So, } \frac{k h}{T k'} = e^{-\frac{\Delta H^\ddagger}{RT}} e^{\frac{\Delta S^\ddagger}{R}}$$

Now

$$\ln\left(\frac{k h}{T k'}\right) = -\frac{\Delta H^\ddagger}{RT} + \frac{\Delta S^\ddagger}{R}$$

Considering  $\frac{h}{k'}$  as constant  $c = 4.79 \times 10^{-11} \text{ s K}$ , where  $h$ =Planck's constant and  $k'$  =Bolzman's constant

Therefore

$$\ln\left(\frac{k}{T} \times c\right) = -\frac{\Delta H^\ddagger}{RT} + \frac{\Delta S^\ddagger}{R}$$

Now from the Eyring plot (Fig. S4)  $\ln\left(\frac{k}{T} \times c\right)$  vs.  $1/T$ , we got slope  $-\frac{\Delta H^\ddagger}{R} = -8.97933 \pm 0.24469$

Therefore,  $\Delta H^\ddagger = 17.84 \pm 0.49 \text{ kcal mol}^{-1}$

Again, we got intercept as  $\frac{\Delta S^\ddagger}{R} = -5.58978 \pm 0.71414$

Therefore,  $\Delta S^\ddagger = -11.11 \pm 1.42 \text{ cal K}^{-1} \text{ mol}^{-1}$

And  $\Delta G^\ddagger = \Delta H^\ddagger - T \Delta S^\ddagger$

Therefore, at 298 K  $\Delta G^\ddagger = 21.15 \pm 0.65 \text{ kcal mol}^{-1}$

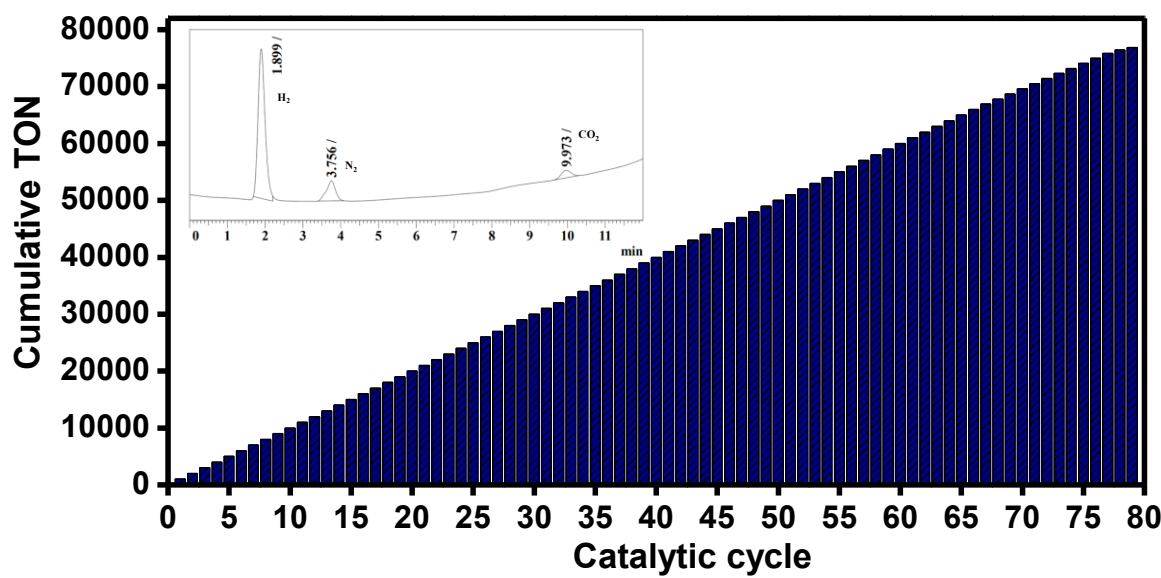


**Fig. S5** Recyclability plot for catalytic FA dehydrogenation over *in situ* **Ru/L7** catalyst. Reaction conditions: FA (0.4 M, 25 mL in water), SF (2.5 mmol), *in situ* **Ru/L7** catalyst (**Ru**: 10  $\mu\text{mol}$ , **L7**: 20  $\mu\text{mol}$ ) at 90°C. FA (380  $\mu\text{L}$ ) was added after each catalytic run. GC-TCD analysis after 80 catalytic runs (inset).

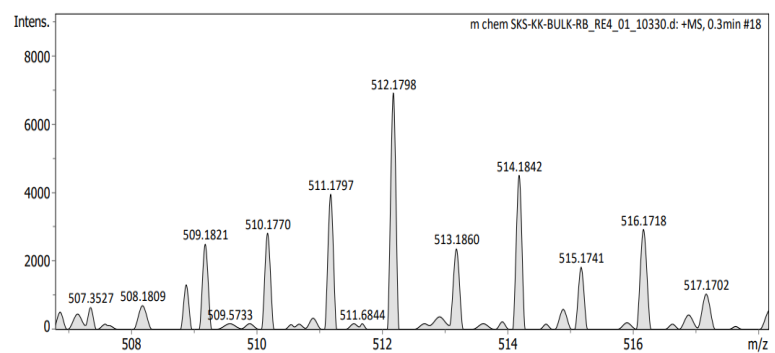
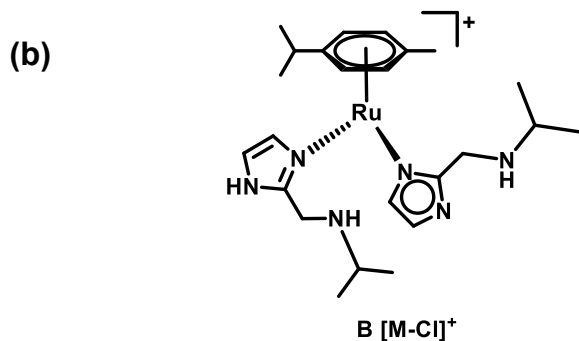
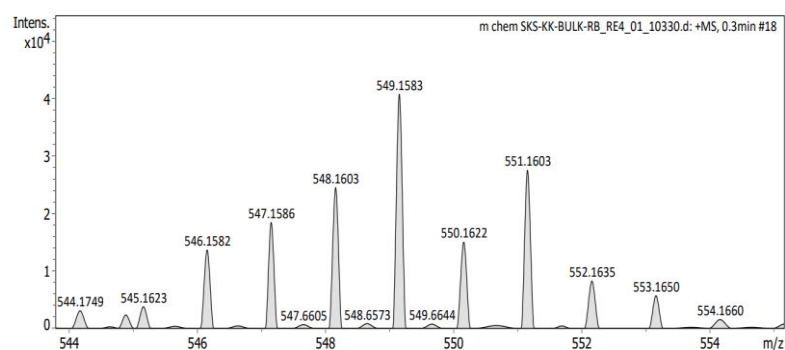
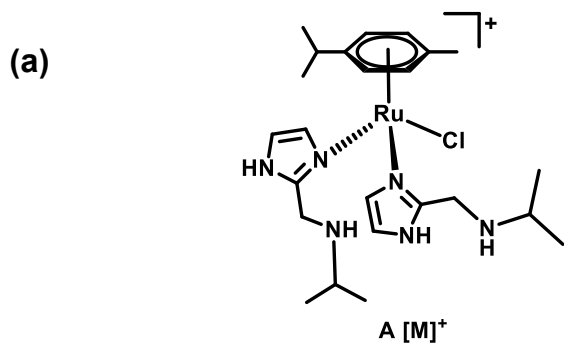


**Fig. S6** Minor Ru/(Ln)<sub>2</sub> species observed after 70 catalytic runs for FA dehydrogenation over Ru/L7 catalyst.

**Table S6** Upscaling the catalytic FA dehydrogenation over *in situ* **Ru/L7** catalyst

Entry	FA (mmol)	Volume of gas (mL)	Time (min)	TON	TOF (h <sup>-1</sup> )
1 <sup>a</sup>	1	49	3	100	2000
2 <sup>b</sup>	10	489	60	1000	1078
3 <sup>c</sup>	20	979	280	2000	530
4 <sup>d</sup>	30	1469	520	3000	471
5 <sup>e</sup>	50	2448	780	5000	451

Reaction conditions: <sup>a</sup>FA (0.4 M, 2.5 mL in water), <sup>b</sup>FA (0.4 M, 25 mL in water), <sup>c</sup>FA (0.4 M, 50 mL in water), <sup>d</sup>FA (0.4 M, 75 mL in water), <sup>e</sup>FA (0.4 M, 120 mL in water), with SF (0.25 equiv. of FA), *in situ* **Ru/L7** catalyst (**Ru**: 10 μmol, **L7**: 20 μmol) at 90°C. TON are calculated the end of the reaction. <sup>a</sup>TOF (initial 3 min). <sup>b-e</sup>TOF (initial 10 min).

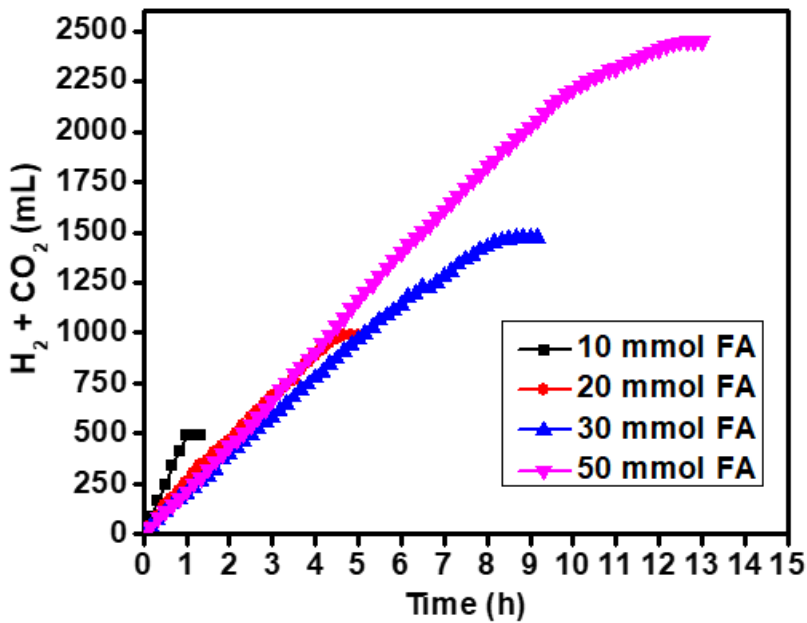


**Fig. S7** Gas evolution plot for upscaling the catalytic FA dehydrogenation over *in situ* Ru/L7 catalyst (**Ru**: 10  $\mu\text{mol}$ , **L7**: 20  $\mu\text{mol}$ ) at 90°C. Reaction conditions: 10 fold: FA (0.4 M, 25 mL in water), SF (2.5 mmol); 20 fold: FA (0.4 M, 50 mL in water), SF (5 mmol); 30 fold: FA (0.4 M, 75 mL in water), SF (7.5 mmol); and 50 fold: FA (0.4 M, 125 mL in water), SF (12.5 mmol).

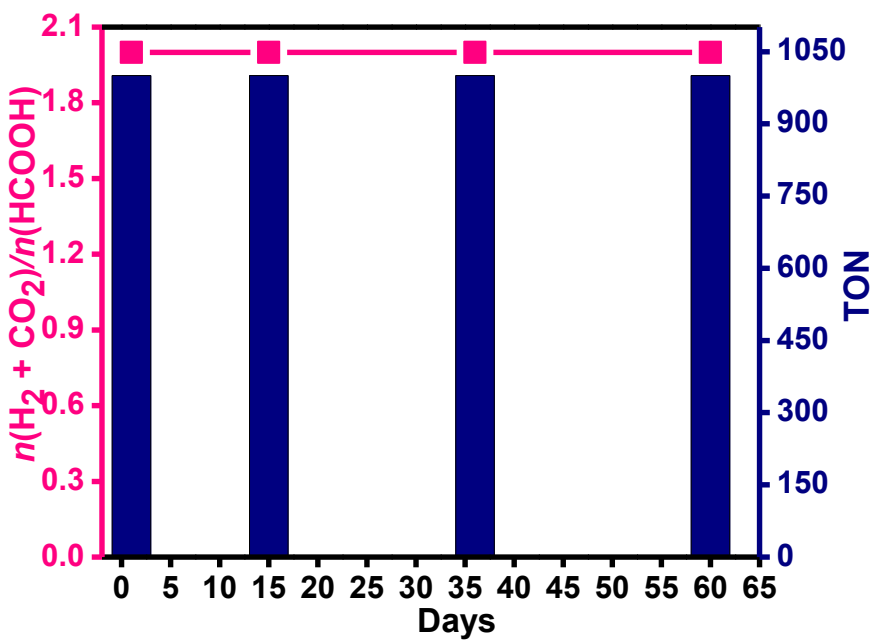


**Fig. S8** Long-term stability of the catalytic FA dehydrogenation over *in situ* Ru/L7 catalyst in water at 90 °C, FA (380  $\mu\text{L}$ ) was added after days 15, 36 and 60 days in the same reaction mixture. Reaction conditions: FA (0.4 M, 25 mL in water), SF (2.5 mmol), *in situ* Ru/L7 catalyst (**Ru**: 10  $\mu\text{mol}$ , **L7**: 20  $\mu\text{mol}$ ) at 90°C.

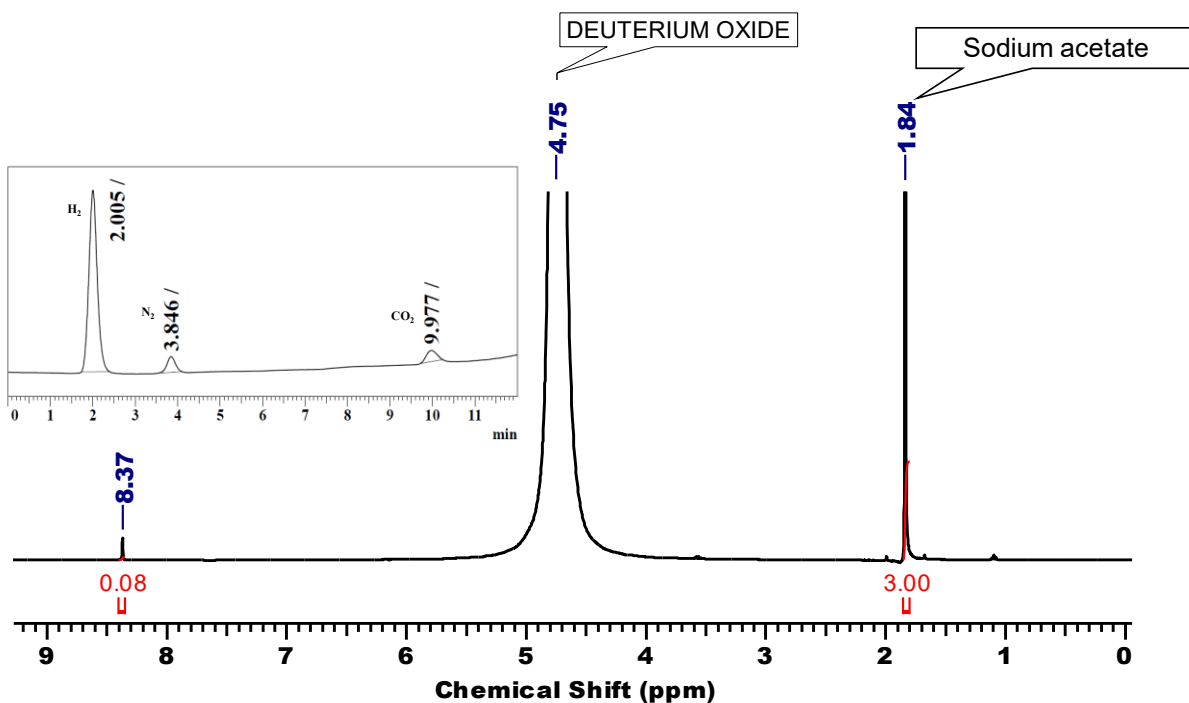


**Fig. S9**  $^1\text{H}$  NMR of reaction aliquot of the catalytic FA dehydrogenation over *in situ* **Ru/L7** catalyst in a high pressure reactor (Closed system) GC-TCD analysis of the evolved gas (inset) Reaction conditions: FA (0.4 M, 25 mL in water), SF (2.5 mmol), *in situ* **Ru/L7** catalyst (**Ru**: 10  $\mu\text{mol}$ , **L7**: 20  $\mu\text{mol}$ ), at 90 °C. NMR yield is calculated by using sodium acetate (0.05 mmol) as internal standard.

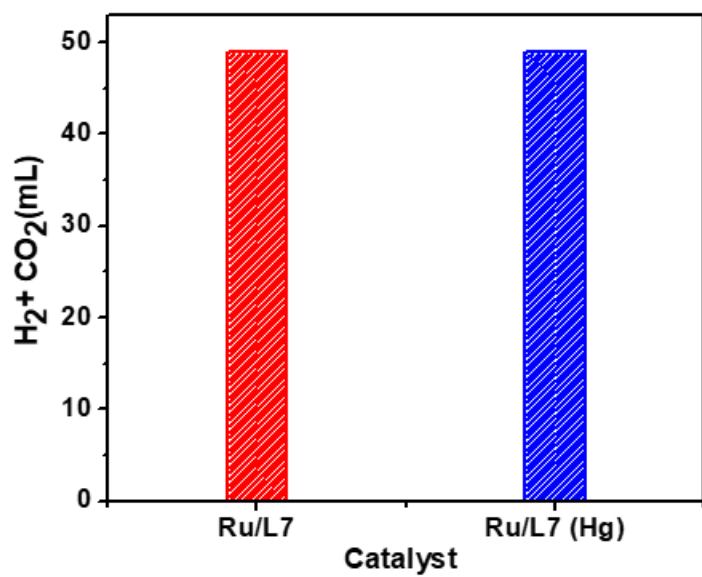


**Fig. S10** Control Hg(0) poisoning experiment, with and without a large excess of elemental Hg(0). Reaction conditions: FA (0.4 M, 2.5 mL in water), *in situ* **Ru/L7** catalyst (**Ru**: 10  $\mu\text{mol}$ , **L7**: 20  $\mu\text{mol}$ ), SF (0.25 mmol), 90 °C.

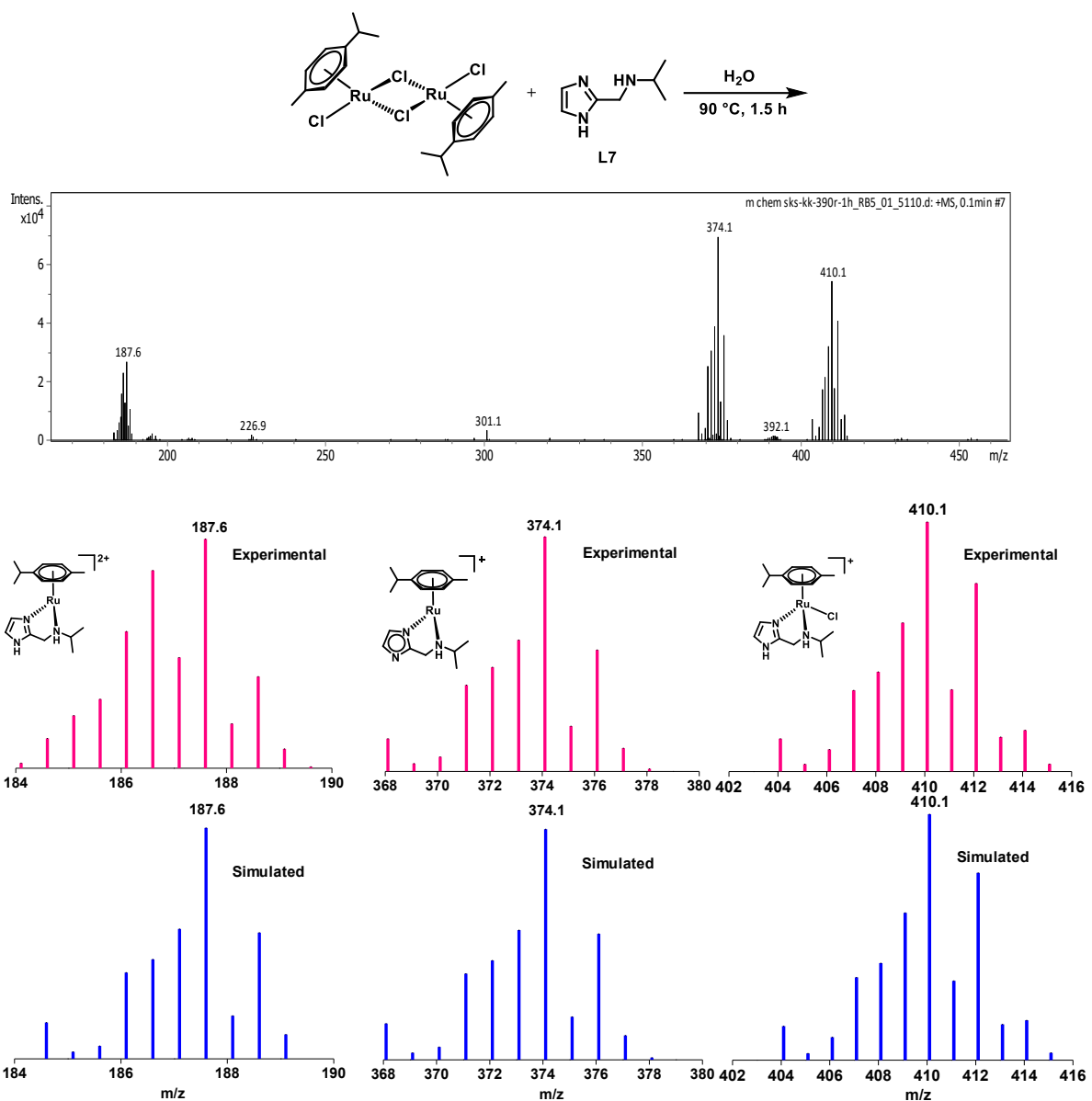


**Fig. S11** Mass analysis of various species formed during the *in situ* generation of **Ru/L7** catalyst. Reaction conditions: **Ru** (10  $\mu\text{mol}$ ), **L7** (20  $\mu\text{mol}$ ),  $\text{H}_2\text{O}$  (2.5 mL), 90 °C, 1.5 h.

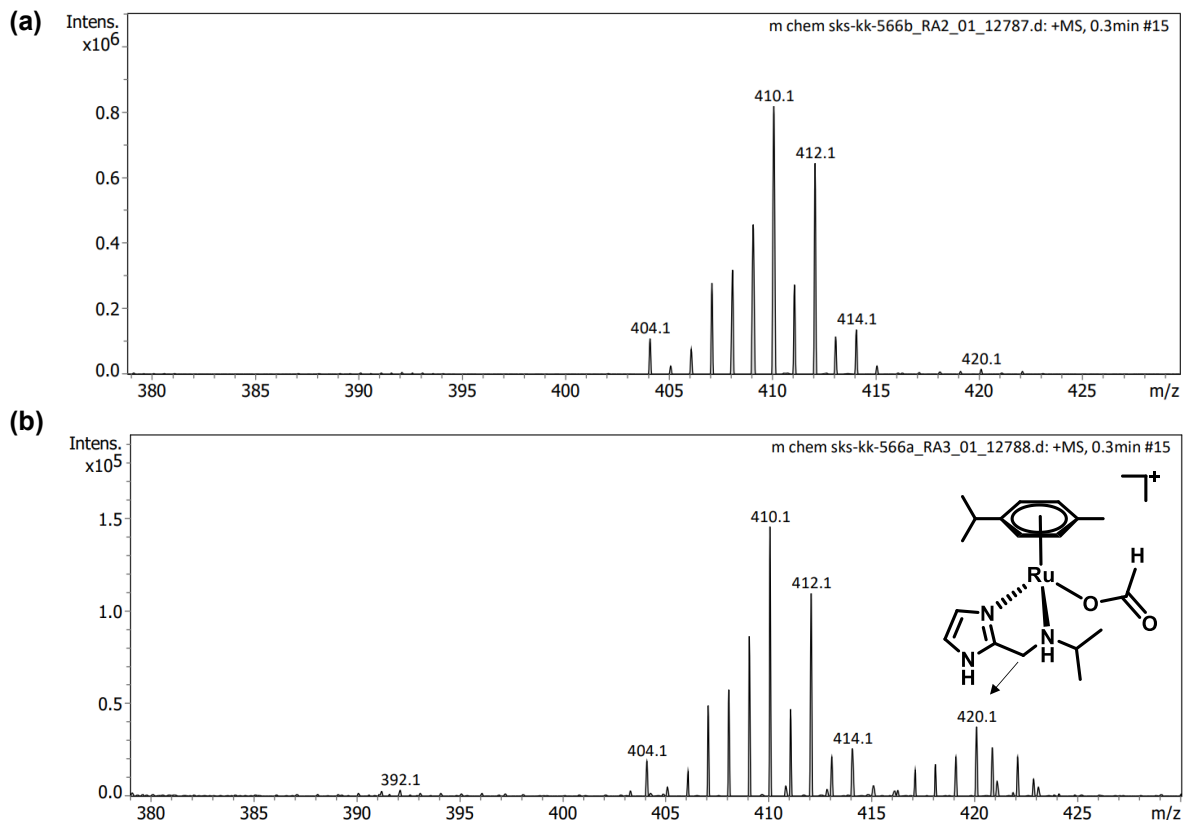
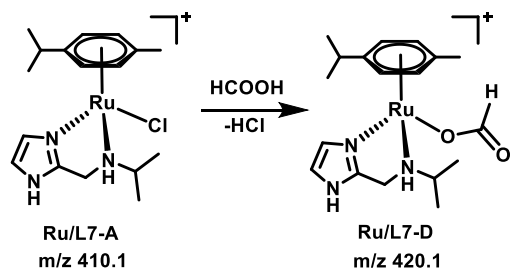


**Fig. S12** Formation Ru-formato species **Ru/L7-B**. (a) Reaction conditions: **Ru** (10  $\mu\text{mol}$ ), **L7** (20  $\mu\text{mol}$ ), FA (1 mmol), H<sub>2</sub>O (2.5 mL), 90 °C, 15 min. (b) Reaction conditions: **Ru** (10  $\mu\text{mol}$ ), **L7** (20  $\mu\text{mol}$ ), FA (1 mmol), SF (0.25 mmol), H<sub>2</sub>O (2.5 mL), 90 °C, 2 min.

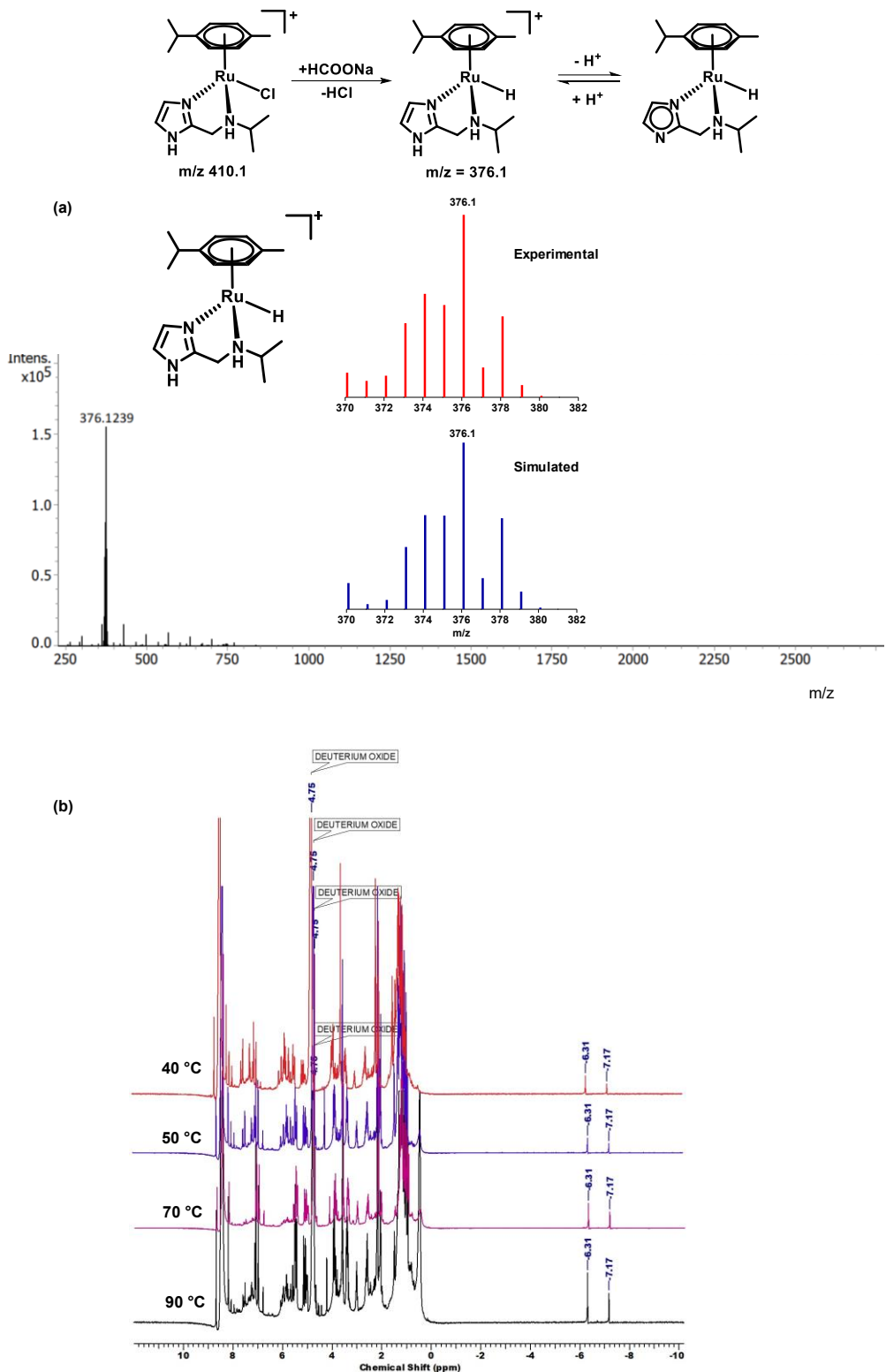


**Fig. S13** (a) Mass analysis of Ru hydrido species **Ru/L7-C**. (b) Temperature dependent <sup>1</sup>H NMR analysis in D<sub>2</sub>O. Reaction conditions: **Ru** (10 µmol), **L7** (20 µmol), SF (1 mmol), D<sub>2</sub>O (2.5 mL), at 40, 50, 70 and 90 °C for 10 min each.

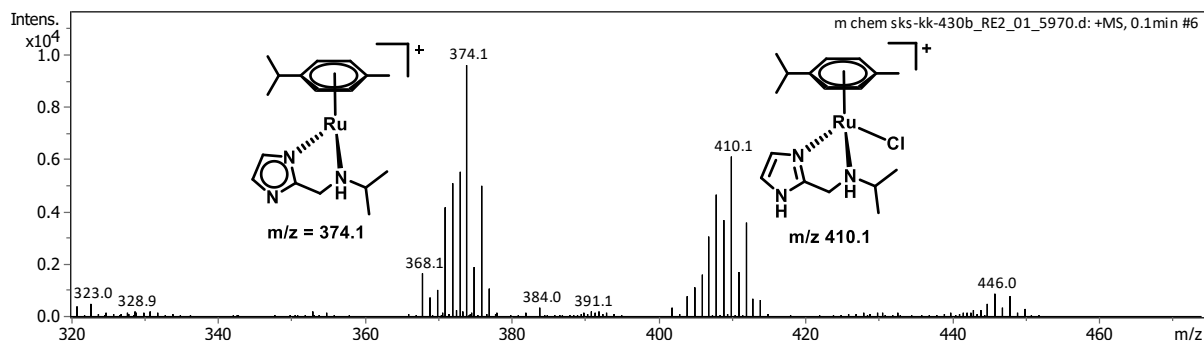
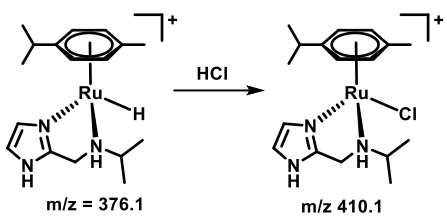


**Fig. S14** Mass investigation of the reaction mixture of *in situ* **Ru** (10  $\mu\text{mol}$ ), **L7** (20  $\mu\text{mol}$ ), treated with SF (1 mmol) in water (2.5 mL) stirred at 90 °C for 10 min in step 1, and further with 1 M HCl (1 mL) in the step 2.

**Table S7** Single crystal X-ray refinement data for **Ru/L7**

Identification Code	<b>Ru/L7</b>
Formula	C <sub>17</sub> H <sub>27</sub> N <sub>3</sub> RuCl <sub>2</sub>
Molecular weight	445.39
Crystal system	triclinic
Space group	P -1
Temperature/K	296
Wavelength	0.71073
a/Å	8.4626(4)
b/Å	8.6713(4)
c/Å	13.9310(7)
α/°	95.566(1)
β/°	102.413(1)
γ/°	92.563(1)
V/ Å <sup>3</sup>	991.41(8)
Z	2
Density/gcm <sup>-1</sup>	1.492
Absorption Coefficient	9.258
Absorption Correction	spherical harmonics- Frame scaling
F(000)	456.0
Total no of reflections	4915
Reflections, I>2σ(I)	4629
Max. 2θ/°	28.278
Ranges (h, k, l)	-11 ≤ h ≤10 -9 ≤ k ≤ 11 -18 ≤ l ≤18
Complete to 2θ (%)	99.7
Refinement method	'SHELXL 2014/7 (Sheldrick, 2015)
Goof (F <sup>2</sup> )	1.039
R indices [I>2σ(I)]	0.0228
R Indices (all data)	0.0246

**Table S8** Selected bond lengths ( $\text{\AA}$ ) for complex **Ru/L7**

Ru1 C11	2.4182(5)
Ru1 N1	2.0773(15)
Ru1 N2	2.1949(15)
Ru1 C2	2.2107(18)
Ru1 C3	2.1771(17)
Ru1 C4	2.1699(18)
Ru1 C5	2.2017(17)
Ru1 C6	2.1754(18)
Ru1 C7	2.1956(18)
N1 C11	1.385(2)
N1 C13	1.328(2)
N2 C14	1.490(2)
N2 C15	1.506(2)
N3 C12	1.380(2)
N3 C13	1.338(2)
C1 C2	1.497(3)
C2 C3	1.411(3)
C2 C7	1.432(3)
C3 C4	1.427(3)
C4 C5	1.409(2)
C5 C6	1.434(3)
C5 C8	1.517(3)
C6 C7	1.403(3)
C8 C9	1.532(3)
C8 C10	1.521(3)
C11 C12	1.363(3)
C13 C14	1.488(3)
C15 C16	1.517(3)
C15 C17	1.525(3)

**Table S9** Selected bond angles ( $^{\circ}$ ) for Ru/L7

N1 Ru1 Cl1	84.30(4)
N1 Ru1 N2	75.16(6)
N1 Ru1 C2	126.10(6)
N1 Ru1 C3	98.32(6)
N1 Ru1 C4	93.77(6)
N1 Ru1 C5	115.32(6)
N1 Ru1 C6	152.12(7)
N1 Ru1 C7	164.00(7)
N2 Ru1 Cl1	87.99(4)
N2 Ru1 C2	93.16(6)
N2 Ru1 C5	169.48(6)
N2 Ru1 C7	101.76(7)
C2 Ru1 Cl1	148.81(5)
C3 Ru1 Cl1	159.91(5)
C3 Ru1 N2	111.98(6)
C3 Ru1 C2	37.51(7)
C3 Ru1 C5	68.76(7)
C3 Ru1 C7	67.93(7)
C4 Ru1 Cl1	121.83(5)
C4 Ru1 N2	147.46(6)
C4 Ru1 C2	68.46(7)
C4 Ru1 C3	38.33(7)
C4 Ru1 C5	37.60(6)
C4 Ru1 C6	68.11(7)
C4 Ru1 C7	80.45(7)
C5 Ru1 Cl1	92.03(5)
C5 Ru1 C2	81.39(7)
C6 Ru1 Cl1	87.71(5)
C6 Ru1 N2	131.28(6)
C6 Ru1 C2	68.29(7)
C6 Ru1 C3	80.72(7)

C6 Ru1 C5	38.25(7)
C6 Ru1 C7	37.45(7)
C7 Ru1 Cl1	111.46(5)
C7 Ru1 C2	37.91(7)
C7 Ru1 C5	68.46(7)
C11 N1 Ru1	136.52(12)
C13 N1 Ru1	115.85(12)
C13 N1 C11	106.74(15)
C14 N2 Ru1	109.76(11)
C14 N2 C15	113.39(15)
C15 N2 Ru1	120.95(11)
C13 N3 C12	107.88(15)
C1 C2 Ru1	130.85(13)
C3 C2 Ru1	69.95(10)
C3 C2 C1	120.92(17)
C3 C2 C7	118.49(17)
C7 C2 Ru1	70.47(11)
C7 C2 C1	120.58(17)
C2 C3 Ru1	72.54(10)
C2 C3 C4	120.54(16)
C4 C3 Ru1	70.56(10)
C3 C4 Ru1	71.11(10)
C5 C4 Ru1	72.43(10)
C5 C4 C3	121.35(16)
C4 C5 Ru1	69.98(10)
C4 C5 C6	117.69(16)
C4 C5 C8	122.48(16)
C6 C5 Ru1	69.88(10)
C6 C5 C8	119.79(16)
C8 C5 Ru1	129.71(12)
C5 C6 Ru1	71.87(10)
C7 C6 Ru1	72.06(10)
C7 C6 C5	121.33(17)

C2 C7 Ru1	71.62(10)
C6 C7 Ru1	70.49(11)
C6 C7 C2	120.57(17)
C5 C8 C9	108.91(16)
C5 C8 C10	113.66(16)
C10 C8 C9	111.5(2)
C12 C11 N1	108.40(16)
C11 C12 N3	106.43(16)
N1 C13 N3	110.55(16)
N1 C13 C14	119.90(16)
N3 C13 C14	129.56(16)
C13 C14 N2	105.87(14)
N2 C15 C16	112.86(17)
N2 C15 C17	111.72(15)
C16 C15 C17	111.35(17)

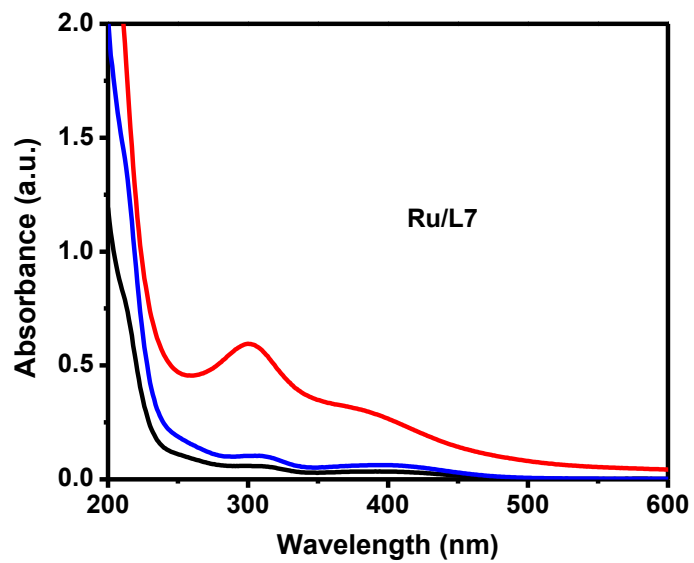


**Fig. S15** UV-vis spectra of (a) aqueous solution of **Ru/L7** (black line), (b) aqueous solution of **Ru/L7** with the addition of SF (red line), and (c) after adding aqueous HCl to an aqueous solution of **Ru/L7** with the addition of SF (blue line).

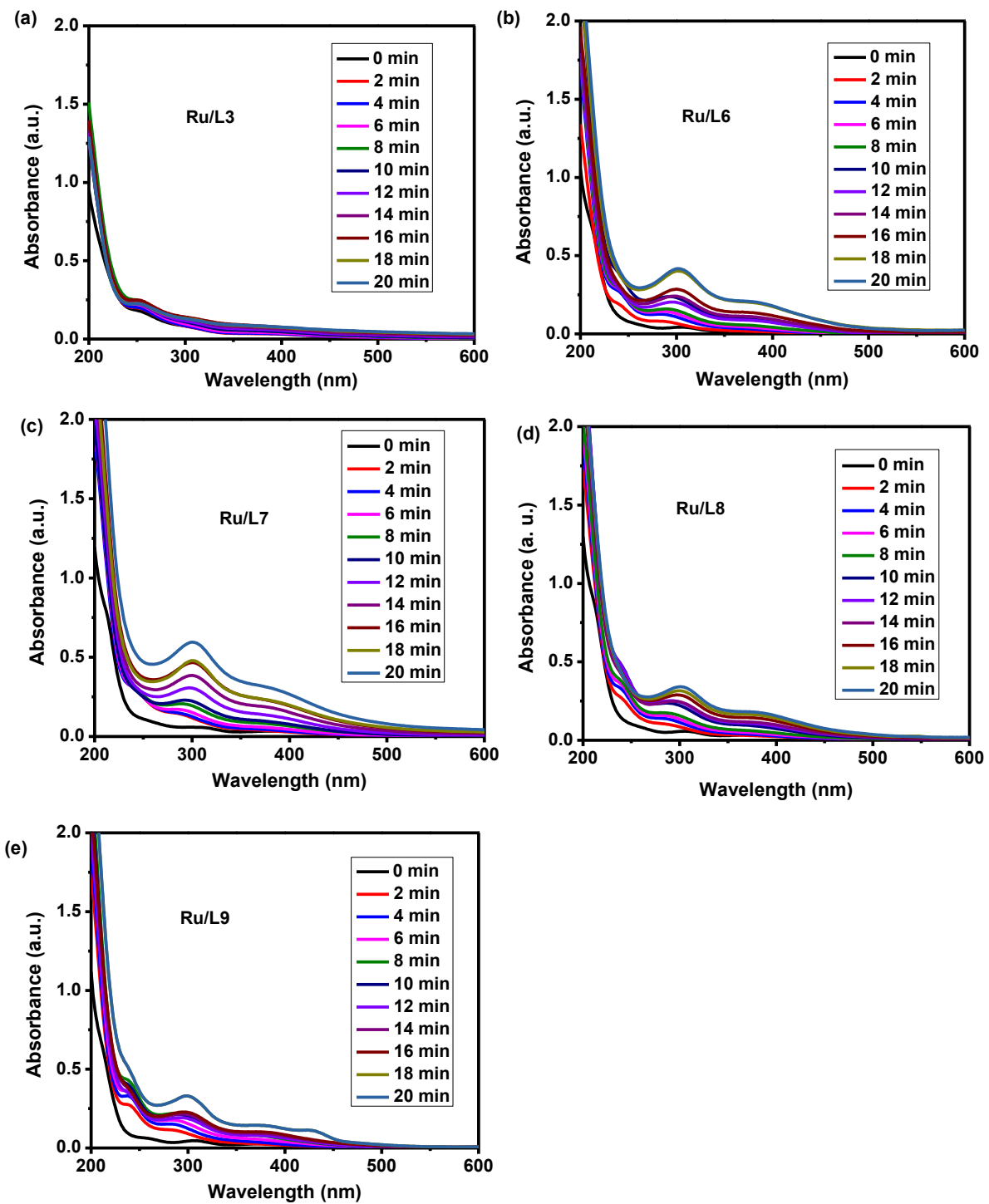


**Fig. S16** UV-vis spectra of aqueous solution of **Ru/Ln** upon the addition of SF.

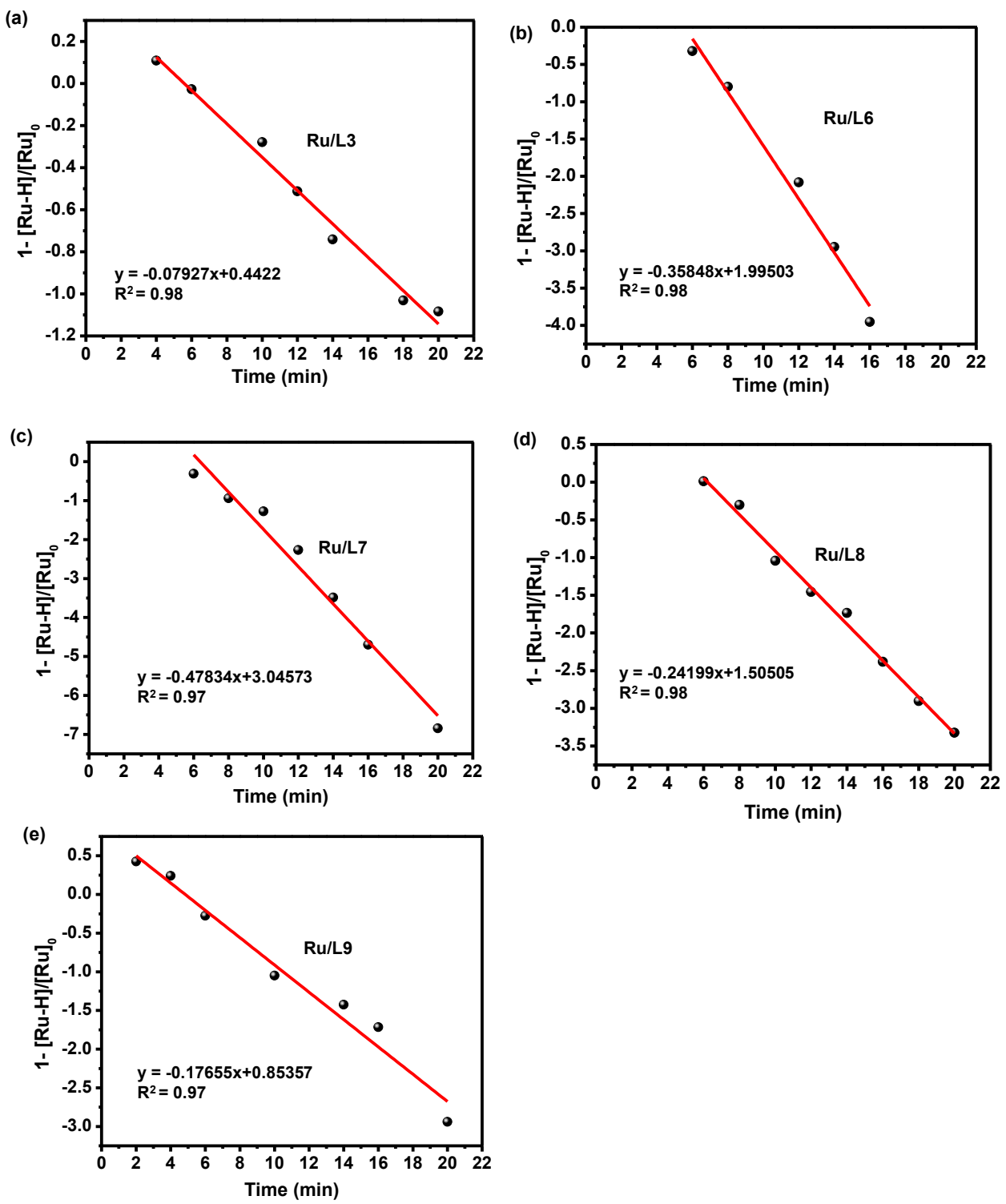


**Fig. S17** Ru-hydride formation rate based on the change in absorption at 400 nm for **Ru/Ln** complexes in the presence of SF.

**Table S10** Ru-hydride formation rates for **Ru/Ln** catalysts in the presence of SF

Catalysts	Hydride formation rate ( $v_{Ru-H} \times 10^{-3}$ $\mu\text{mol s}^{-1}$ )
<b>Ru/L3</b>	1.3
<b>Ru/L6</b>	5.9
<b>Ru/L7</b>	8.0
<b>Ru/L8</b>	4.0
<b>Ru/L9</b>	2.9

## CO<sub>2</sub> capture and hydrogenation

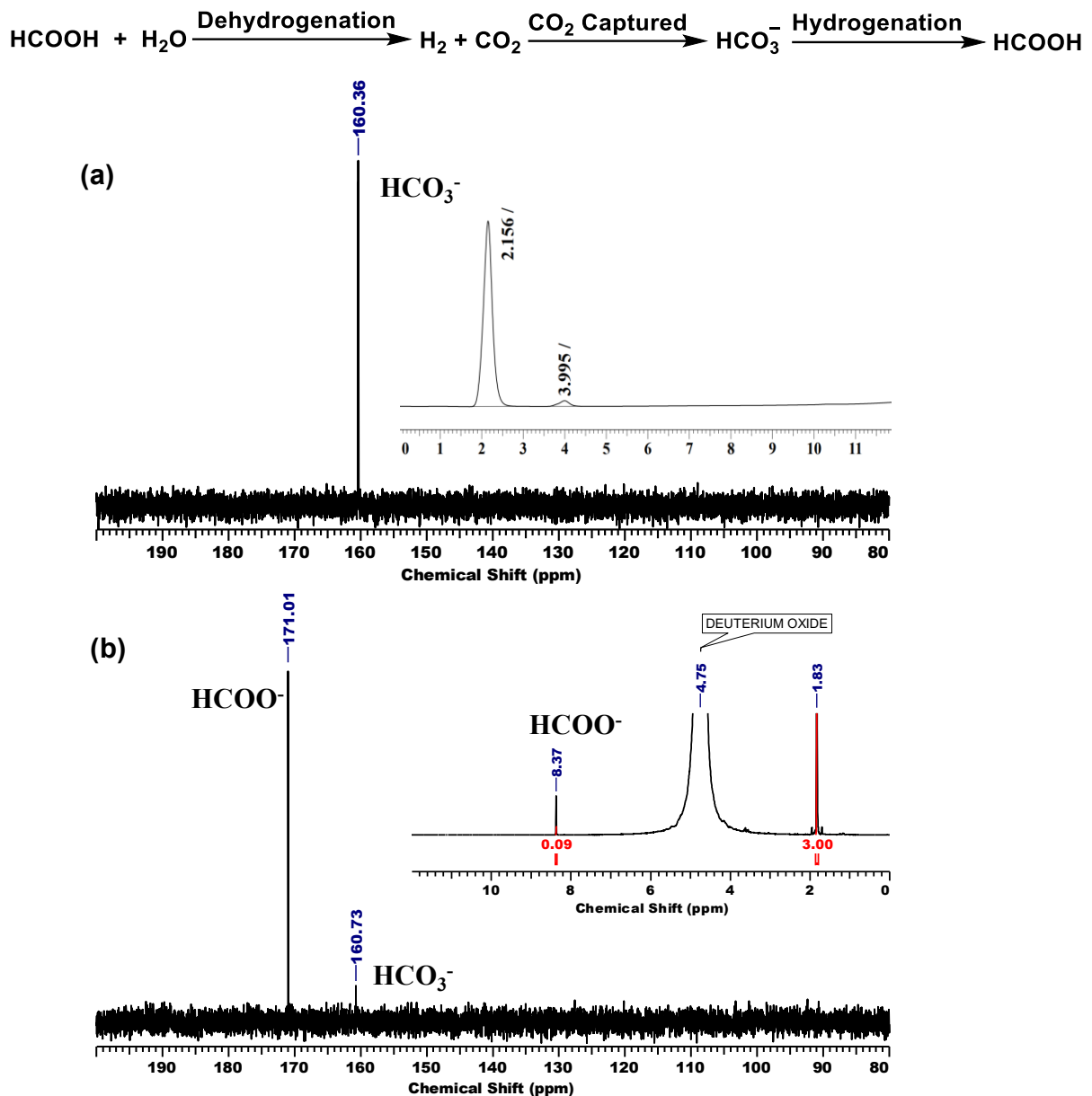


**Fig. S18** CO<sub>2</sub> capture and hydrogenation. **Dehydrogenation** of FA, Reaction conditions: Reaction conditions: FA (0.4 M, 25 mL in water), *in situ* Ru/L7 catalyst (Ru: 10  $\mu\text{mol}$ , L7: 20  $\mu\text{mol}$ ), SF (2.5 mmol), 90 °C. **CO<sub>2</sub> captured** (a) <sup>13</sup>C NMR of CO<sub>2</sub> captured reaction aliquot (5 mL of 2 M KOH), GC TCD analysis of effluent gas (inset). **Hydrogenation** of bicarbonate, Reaction conditions: *in situ* Ru/L7 catalyst (Ru: 10  $\mu\text{mol}$ , L7: 20  $\mu\text{mol}$ ), H<sub>2</sub> (20 bar), 80 °C, 48 h. (b) <sup>1</sup>H (inset) and <sup>13</sup>C NMR (in D<sub>2</sub>O) of reutilization of captured CO<sub>2</sub> reaction aliquot (hydrogenation of HCO<sub>3</sub><sup>-</sup>).

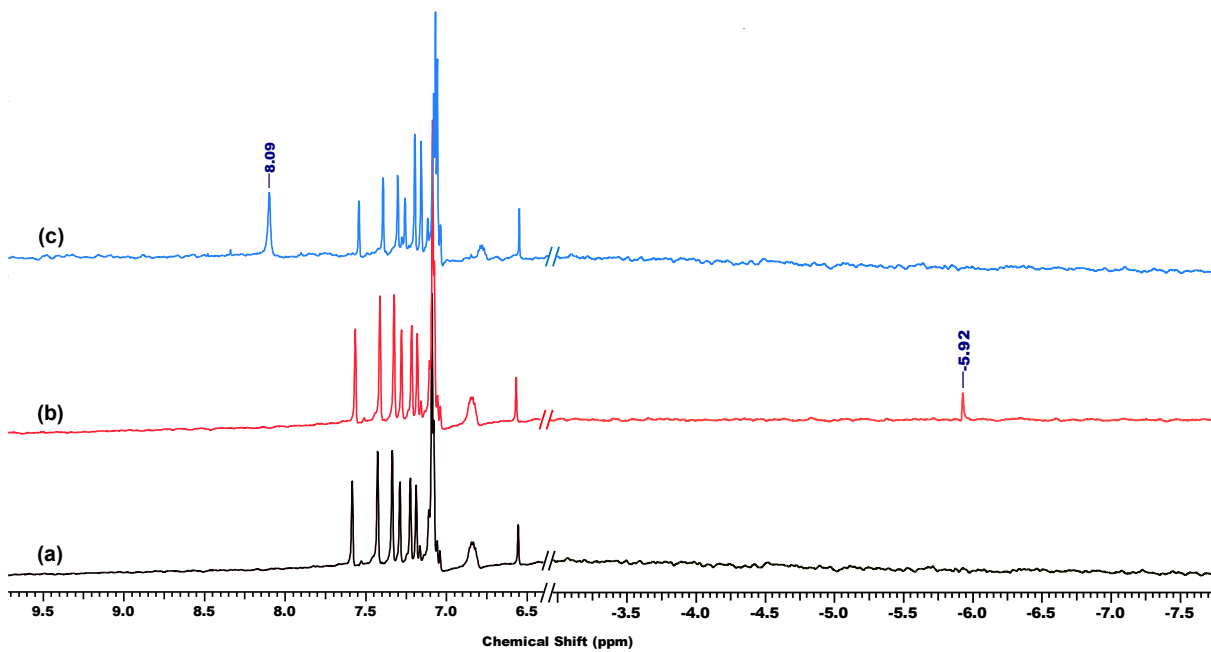


**Fig. S19** <sup>1</sup>H NMR spectrum (in DMSO-d<sub>6</sub>) for generation of Ru-hydrido species and Ru-formato species involved in CO<sub>2</sub> hydrogenation. Reaction conditions: (a) *ex situ* Ru/L7 (0.02 mmol) in DMSO (1.5 mL). (b) Ru/L7 (0.02 mmol) in DMSO (1.5 mL), H<sub>2</sub> (20 bar), 80 °C, 2.5 h. (c) *ex situ* Ru/L7 (0.02 mmol) in DMSO (1.5 mL), H<sub>2</sub> (10 bar), CO<sub>2</sub> (10 bar), 80 °C, 2.5 h.

## **General Procedure for the Synthesis of Ligands (L2 -L9)**

### **L2**

Ligand **L2** is synthesized by reducing 2-thiophenecarboxaldehyde (5 mmol, 0.5 mL) with NaBH<sub>4</sub> (7 mmol, 265 mg) in 15 mL of methanol at room temperature for 2 h. Completion of the reaction is monitored by thin layer chromatography. Further, all the volatiles are removed under reduced pressure, followed by extraction with dichloromethane (3 × 15 mL)/water. Then, the organic layer is dried over anhydrous Na<sub>2</sub>SO<sub>4</sub>, and further the solvent was evaporated under reduced pressure to get the desired oily product (70% yield). <sup>1</sup>H NMR (500 MHz, CDCl<sub>3</sub>): δ (ppm) 7.27-7.26 (d, J = 5 Hz, 1H), 6.99-6.97 (m, 2H), 4.78 (s, 2H), 2.35 (s, 1H); <sup>13</sup>C NMR (125 MHz, CDCl<sub>3</sub>): δ (ppm) 144.18, 127.07, 125.80, 125.69, 60.14.

### **L3**

Ligand **L3** is synthesized by reducing 2-imidazolecarboxaldehyde (5 mmol, 480 mg) with NaBH<sub>4</sub> (2.5 mmol, 95 mg) in 15 mL of ethanol at room temperature for 2 h. Completion of the reaction is monitored by thin layer chromatography. Further, all the volatiles are removed under reduced pressure then the product is recrystallized with diethyl ether in methanol to obtain the desired pure product (72% yield). <sup>1</sup>H NMR: (500 MHz, DMSO-d<sub>6</sub>) δ (ppm) 11.86 (s, 1H), 6.90 (s, 2H), 5.29 (s, 1H), 4.44 (s, 2H); <sup>13</sup>C NMR (125 MHz, DMSO-d<sub>6</sub>) δ 147.95, 122.04, 57.03.

### **L4**

Ligand **L4** is synthesized by condensation of furfural (5 mmol, 0.414 mL) with n-propylamine (25 mmol, 2.1 mL) for 12h, followed by reduction with NaBH<sub>4</sub> (5.1 mmol, 193 mg) in 15 mL of ethanol at room temperature for 2 h. Completion of the reaction is monitored by thin layer chromatography. Further, all the volatiles are removed under reduced pressure, followed by extraction with dichloromethane (3 × 15 mL)/water. Then, the organic layer is dried over anhydrous Na<sub>2</sub>SO<sub>4</sub>, and further the solvent was evaporated under reduced pressure to get the desired oily product (75 % yield). <sup>1</sup>H NMR (500 MHz, CDCl<sub>3</sub>): δ (ppm) 7.36 (s, 1H), 6.31(s, 1H), 6.18 (s, 1H), 3.78 (s, 2H), 2.60-2.57 (t, *J*<sub>1</sub> =10 Hz, *J*<sub>2</sub> = 5 Hz, 2H), 1.80 (s, 1H), 1.54-1.49 (m, 2H), 0.93-0.90 (t, *J*<sub>1</sub> = 10 Hz, *J*<sub>2</sub> = 5 Hz, 3H); <sup>13</sup>C NMR (125 MHz, CDCl<sub>3</sub>): δ (ppm) 153.94, 141.71, 110.04, 106.77, 50.98, 46.13, 22.99, 11.70. HRMS calcd for [M + H]<sup>+</sup> [C<sub>8</sub>H<sub>13</sub>NO] 140.1070, observed 140.1098

### **L5**

Ligand **L5** is synthesized by condensation of 2-thiophenecarboxaldehyde (5 mmol, 0.5 mL) with n-propylamine (25 mmol, 2.1 mL) for 12 h, followed by reduction with NaBH<sub>4</sub> (5.1 mmol, 193 mg) in 15 mL of ethanol at room temperature for 2 h. Completion of the reaction is monitored by thin layer chromatography. Further, all the volatiles are removed under reduced pressure, followed by extraction with dichloromethane (3 × 15 mL)/water. Then, the organic layer is dried over anhydrous Na<sub>2</sub>SO<sub>4</sub>, and further the solvent was evaporated under reduced pressure to get the desired oily product (75 % yield). <sup>1</sup>H NMR (500 MHz, CDCl<sub>3</sub>): δ (ppm) 7.22-7.21 (d, *J* = 5 Hz, 1H), 6.96-6.94 (m, 2 H), 4.00 (s, 2H), 2.65-2.63 (t, *J* = 5 Hz, 2 H), 1.70 (s, 1H), 1.58-1.51 (m, 2H), 0.95-0.92 (t, *J*<sub>1</sub> = 10 Hz, *J*<sub>2</sub> = 5 Hz, 3H); <sup>13</sup>C NMR (125 MHz, CDCl<sub>3</sub>): δ (ppm) 143.91, 126.31, 124.54, 123.99, 50.72, 48.05, 22.75, 11.46. HRMS calcd for [M + H]<sup>+</sup> [C<sub>8</sub>H<sub>13</sub>NS] 156.0841, observed 156.0851.

## L6

Ligand **L6** is synthesized by condensation of with 2-imidazolecarboxaldehyde (4 mmol, 384.24 mg) with n-propylamine (20 mmol, 1.6 mL) for 12 h, followed by reduction with NaBH<sub>4</sub> (2.5 mmol, 95 mg) in 25 mL of methanol at room temperature for 2 h. Completion of the reaction is monitored by thin layer chromatography. Further, all the volatiles are removed under reduced pressure, followed by extraction with dichloromethane (3 × 15 mL)/water. Then, the organic layer is dried over anhydrous Na<sub>2</sub>SO<sub>4</sub>, and further the solvent was evaporated under reduced pressure to get the desired oily product (78 % yield). <sup>1</sup>H NMR (500 MHz, CDCl<sub>3</sub>): δ (ppm) 6.96 (s, 2H), 3.89 (s, 2H), 2.61-2.58 (t, *J*<sub>1</sub> = 5 Hz, *J*<sub>2</sub> = 10 Hz, 2H), 1.54-1.48 (m, 2H), 0.92-0.89 (t, *J*<sub>1</sub> = 10 Hz, *J*<sub>2</sub> = 5 Hz, 3H); <sup>13</sup>C NMR (125 MHz, CDCl<sub>3</sub>): δ (ppm) 147.22, 122.01, 51.71, 47.24, 23.12, 11.87. HRMS calcd for [M + H]<sup>+</sup> [C<sub>7</sub>H<sub>13</sub>N<sub>3</sub>] 140.1182, observed 140.1199.

## L7

Ligand **L7** is synthesized by condensation of with 2-imidazolecarboxaldehyde (4 mmol, 384.24 mg) with iso-propylamine (20 mmol, 1.7 mL) for 12 h, followed by reduction with NaBH<sub>4</sub> (2.5 mmol, 95 mg) in 25 mL of methanol at room temperature for 2 h. Completion of the reaction is monitored by thin layer chromatography. Further, all the volatiles are removed under reduced pressure, followed by extraction with dichloromethane (3 × 15 mL)/water. Then, the organic layer is dried over anhydrous Na<sub>2</sub>SO<sub>4</sub>, and further the solvent was evaporated under reduced pressure to get the desired oily product (80 % yield). <sup>1</sup>H NMR (500 MHz, CDCl<sub>3</sub>): δ (ppm) 6.95 (s, 2H), 3.89 (s, 2H), 2.87-2.81 (m, 1H), 1.08-1.07 (d, *J* = 5 Hz, 6H); <sup>13</sup>C NMR (125 MHz, CDCl<sub>3</sub>): δ (ppm) 146.90, 121.41, 48.57, 44.51, 22.38. HRMS calcd for [M + H]<sup>+</sup> [C<sub>7</sub>H<sub>13</sub>N<sub>3</sub>] 140.1182, observed 140.1198.

## L8

Ligand **L8** is synthesized by condensation of with 2-imidazolecarboxaldehyde (4 mmol, 384.24 mg) with n-butylamine (10 mmol, 0.98 mL) for 12 h, followed by reduction with NaBH<sub>4</sub> (2.5 mmol, 95 mg) in 25 mL of methanol at room temperature for 2 h. Completion of the reaction is monitored by thin layer chromatography. Further, all the volatiles are removed under reduced pressure, followed by extraction with dichloromethane (3 × 15 mL)/water. Then, the organic layer is dried over anhydrous Na<sub>2</sub>SO<sub>4</sub>, and further the solvent was evaporated under reduced pressure to get the desired oily product (73 % yield). <sup>1</sup>H NMR (500 MHz, CDCl<sub>3</sub>): δ (ppm) 6.97 (s, 2H), 3.90 (s, 2H), 2.65-2.62 (t, *J*<sub>1</sub> = 10 Hz, *J*<sub>2</sub> = 5 Hz, 2 H), 1.50-1.44 (m, 2H), 1.37-1.30 (m, 2H), 0.91-0.89 (t, *J* = 5 Hz, 3H); <sup>13</sup>C NMR (125 MHz, CDCl<sub>3</sub>): δ (ppm) 146.96, 122.07, 49.52, 47.21, 32.02, 31.14, 20.55, 14.12. HRMS calcd for [M + H]<sup>+</sup> [C<sub>8</sub>H<sub>15</sub>N<sub>3</sub>] 154.1339, observed 154.1351.

## L9

Ligand **L9** is synthesized by condensation of with 2-imidazolecarboxaldehyde (4 mmol, 384.24 mg) with iso-butylamine (15 mmol, 1 mL) for 12 h, followed by reduction with NaBH<sub>4</sub> (2.5 mmol, 95 mg) in 10 mL of ethanol at room temperature for 2 h. Completion of the reaction is monitored by thin layer chromatography. Further, all the volatiles are removed under reduced pressure, followed by extraction with dichloromethane (3 × 15 mL)/water. Then, the organic layer is dried over anhydrous Na<sub>2</sub>SO<sub>4</sub>, and further the solvent was evaporated under reduced pressure to get the desired oily product (76 % yield). <sup>1</sup>H NMR (500 MHz, CDCl<sub>3</sub>): δ (ppm) 6.95 (s, 2H), 5.64 (s, 2H), 3.87 (s, 2H) 2.43-2.42 (d, *J* = 5 Hz, 2 H), 1.77-1.69 (m, 1H), 0.89-0.87 (d, *J* = 10 Hz, 6H); <sup>13</sup>C NMR (125 MHz, CDCl<sub>3</sub>): δ (ppm) 147.12, 121.99, 57.71, 47.27, 28.32, 20.74. HRMS calcd for [M + H]<sup>+</sup> [C<sub>8</sub>H<sub>15</sub>N<sub>3</sub>] 154.1339, observed 154.1352.

### Synthesis of [(η<sup>6</sup>-C<sub>10</sub>H<sub>14</sub>)Ru(L7)Cl]<sup>+</sup> (Ru/L7)

*Ex situ* **Ru/L7** catalyst is synthesized by treating [(η<sup>6</sup>-C<sub>10</sub>H<sub>14</sub>)RuCl<sub>2</sub>]<sub>2</sub> (0.05 mmol, 30.6 mg) and **L7** (0.12 mmol, 16.7 mg) in acetonitrile (15 mL) under reflux for 12 h. The volume of the reaction mixture is reduced to 1 mL under reduced pressure, followed by precipitation with excess of diethyl ether to obtain yellow solid. The identity of the synthesised *ex situ* complex is confirmed by NMR, HRMS and single-crystal X-ray diffraction. <sup>1</sup>H NMR (400 MHz, DMSO-d<sub>6</sub>): δ (ppm) 13.04 (s, NH), 7.63 (s, 1H), 7.31 (s, 1H), 5.88-5.87 (d, *J* = 4 Hz, 2H), 5.69-5.68 (d, *J* = 4 Hz, 2H), 3.70-3.65 (m, 1H), 3.26-3.19 (m, 2H), 2.85-2.79 (m, 1H), 2.05 (s, 3H), 1.18-1.16 (d, *J* = 8 Hz, 3H), 1.14-1.12 (d, *J* = 8 Hz, 3H), 0.94-0.91 (m, 6H); <sup>13</sup>C NMR (100 MHz, DMSO-d<sub>6</sub>): δ (ppm) 149.33, 128.61, 118.57, 104.27, 82.86, 81.85, 81.31, 80.42, 50.33, 30.28, 27.71, 20.88, 19.79, 17.40, 13.83. HRMS calcd for [M]<sup>+</sup> [C<sub>17</sub>H<sub>27</sub>N<sub>3</sub>RuCl] 410.0933, observed 410.0944.

## Characterization of ligand L2-L9 and metal complexes (Ru/L7)

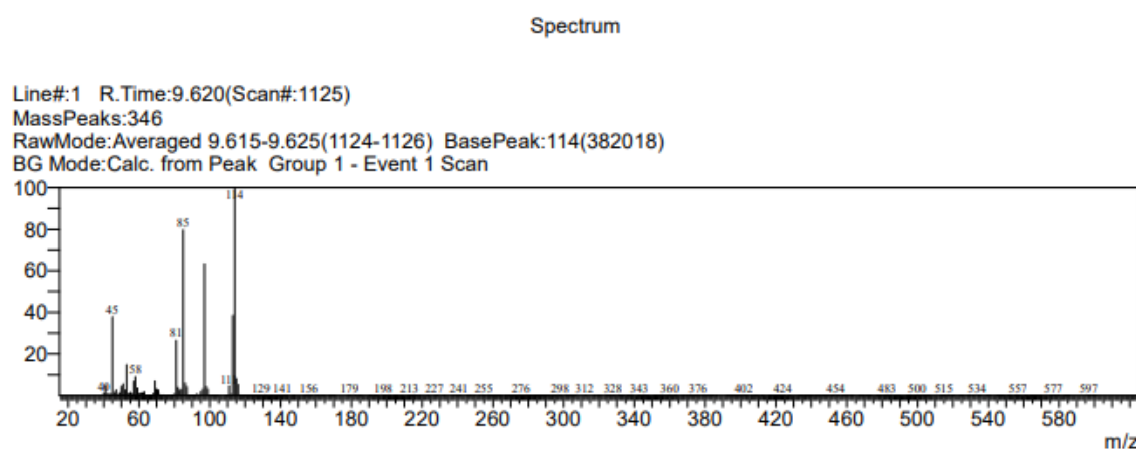
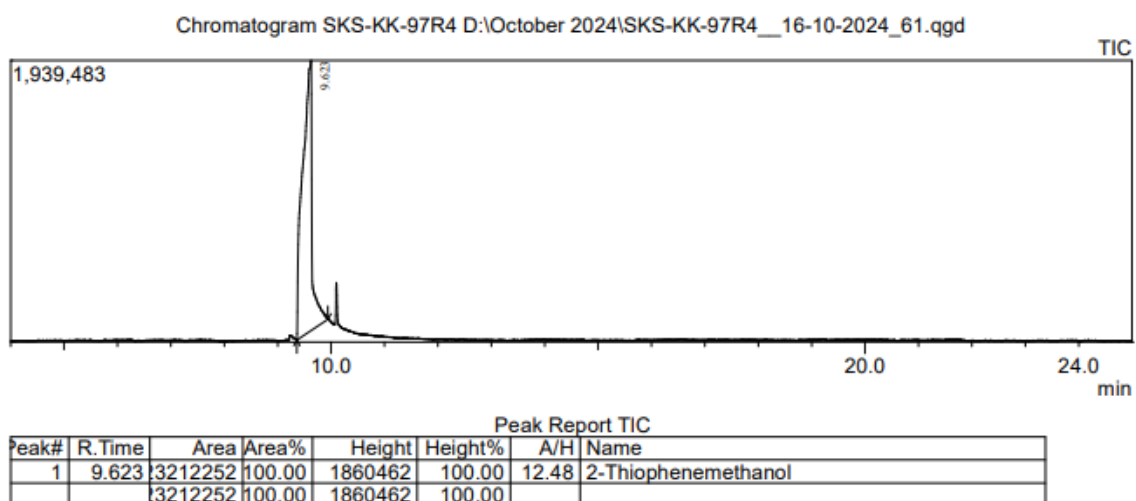


**Fig. S20** GC-MS data of L2

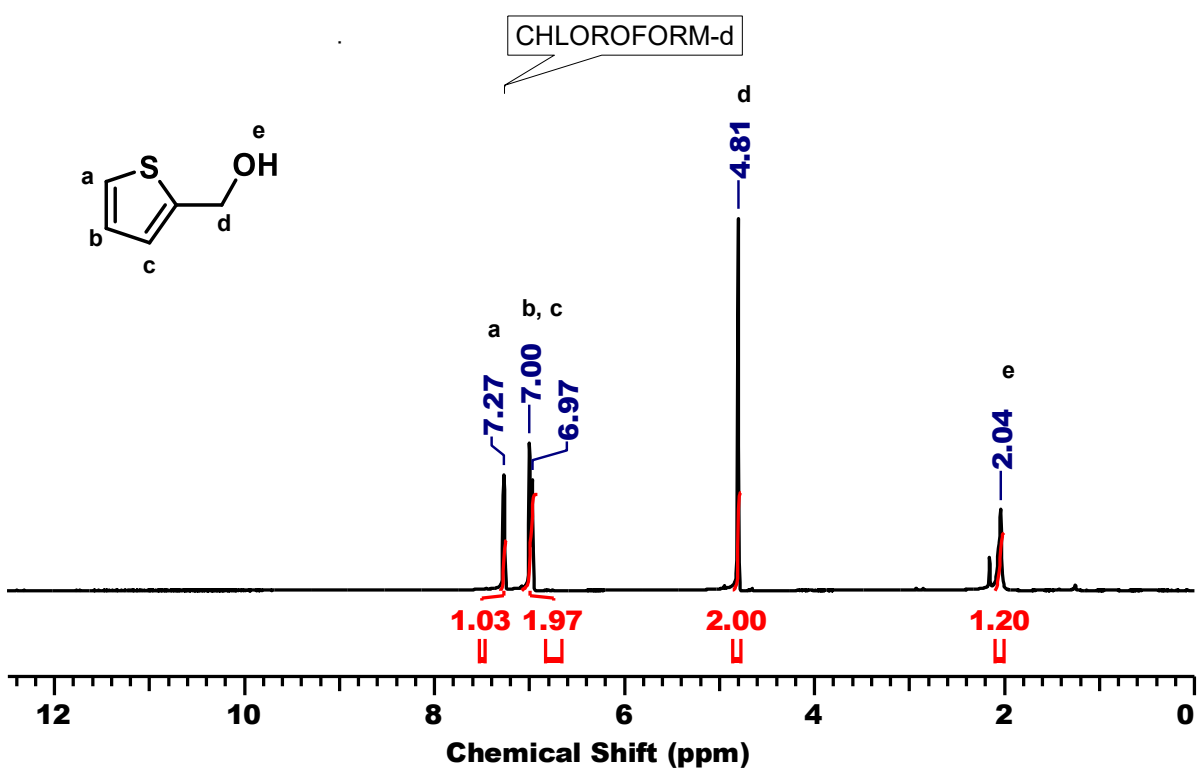


Fig. S21  $^1\text{H}$  NMR of L2

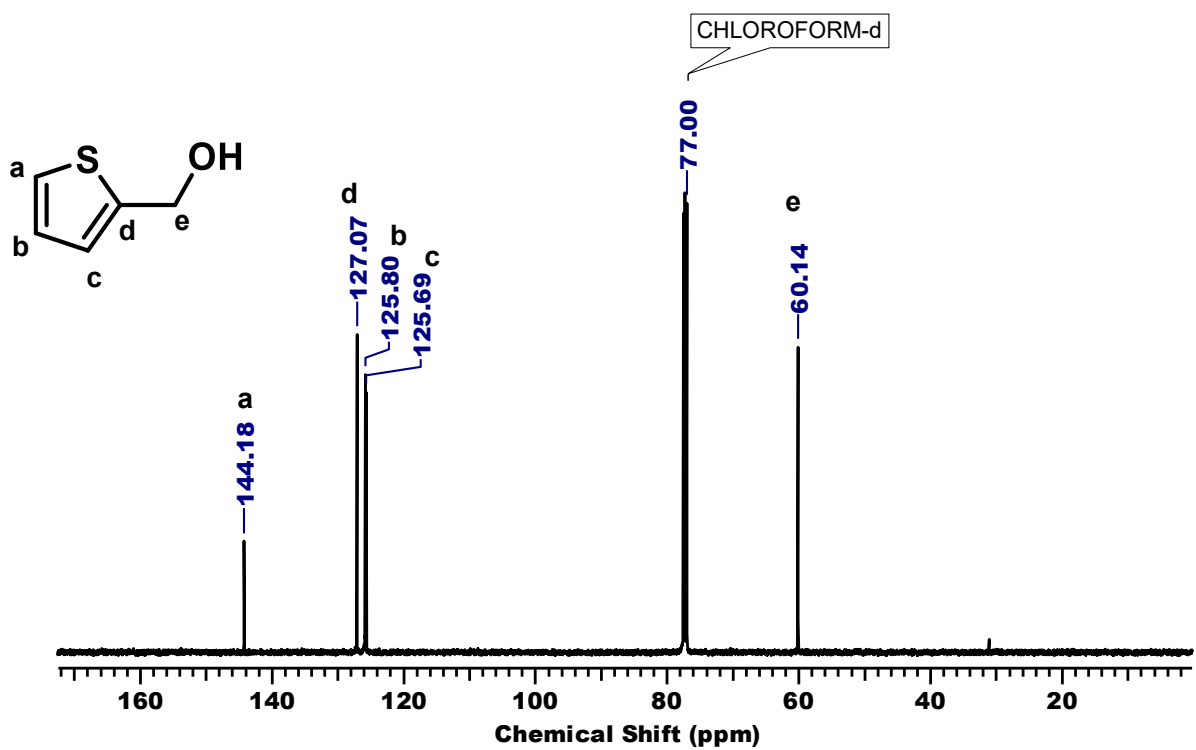
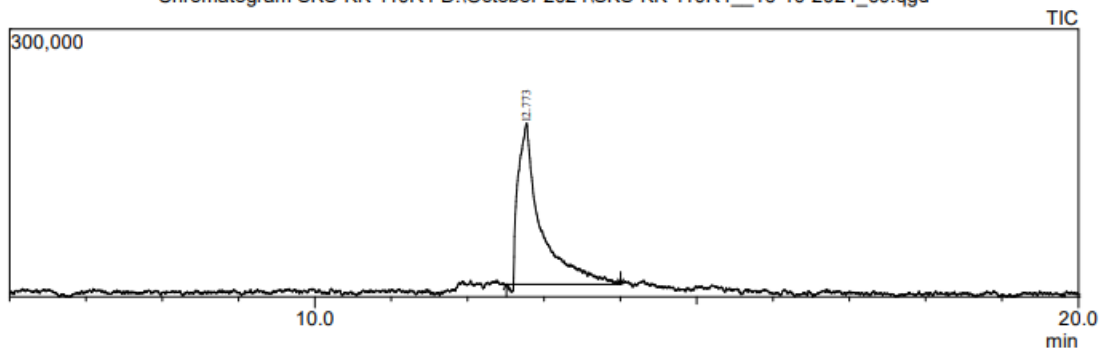
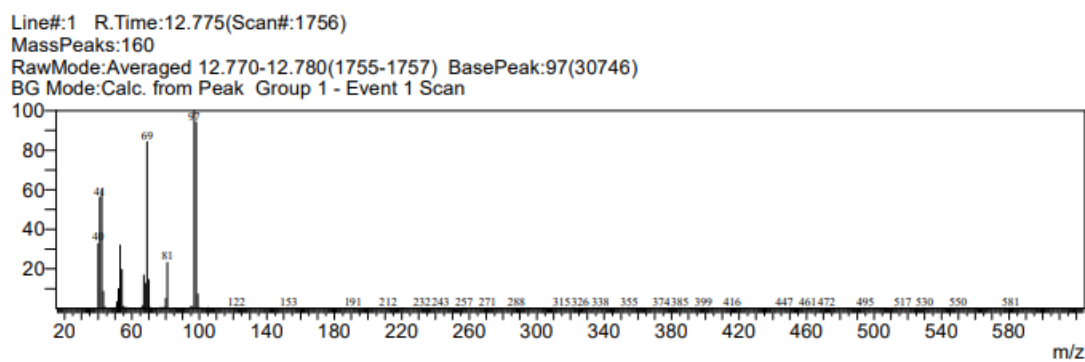


Fig. S22  $^{13}\text{C}$  NMR of L2



Peak Report TIC							
Peak#	R.Time	Area	Area%	Height	Height%	A/H	Name
1	12.773	3606165	100.00	177172	100.00	20.35	1H-Imidazole-2-methanol
		3606165	100.00	177172	100.00		

Spectrum

**Fig. S23** GC-MS data of L3

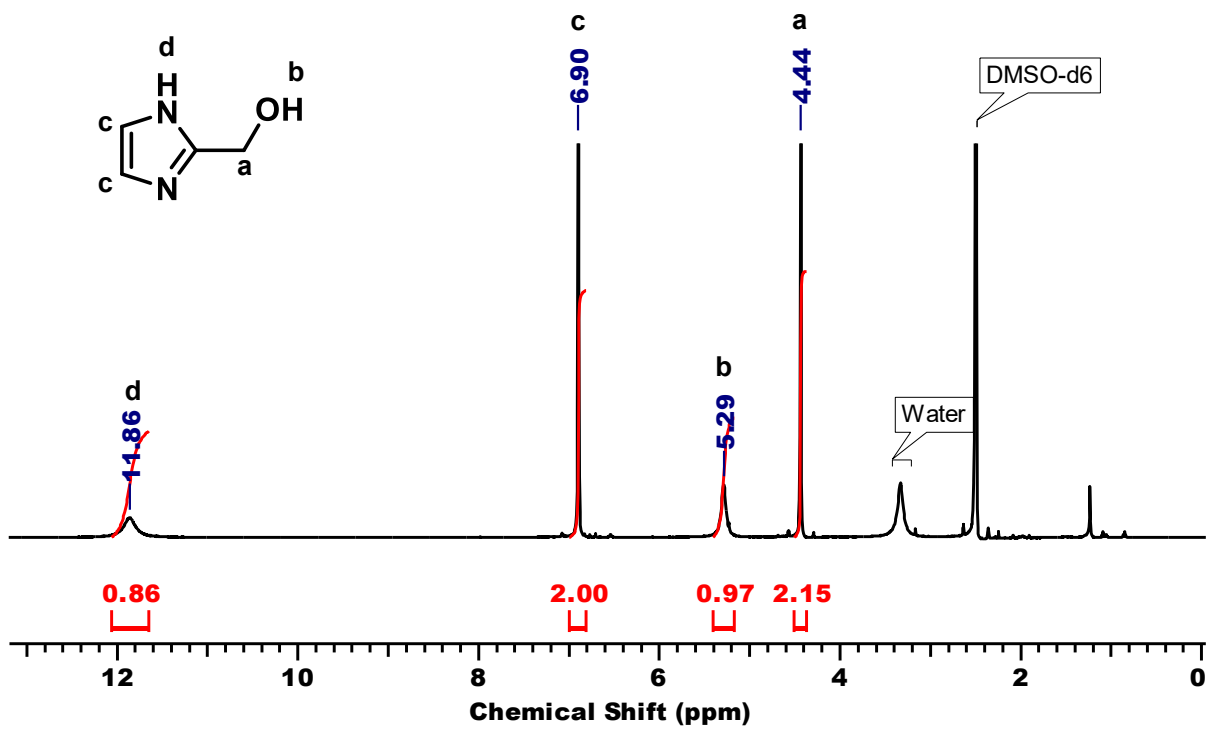


Fig. S24  $^1\text{H}$  NMR of L3

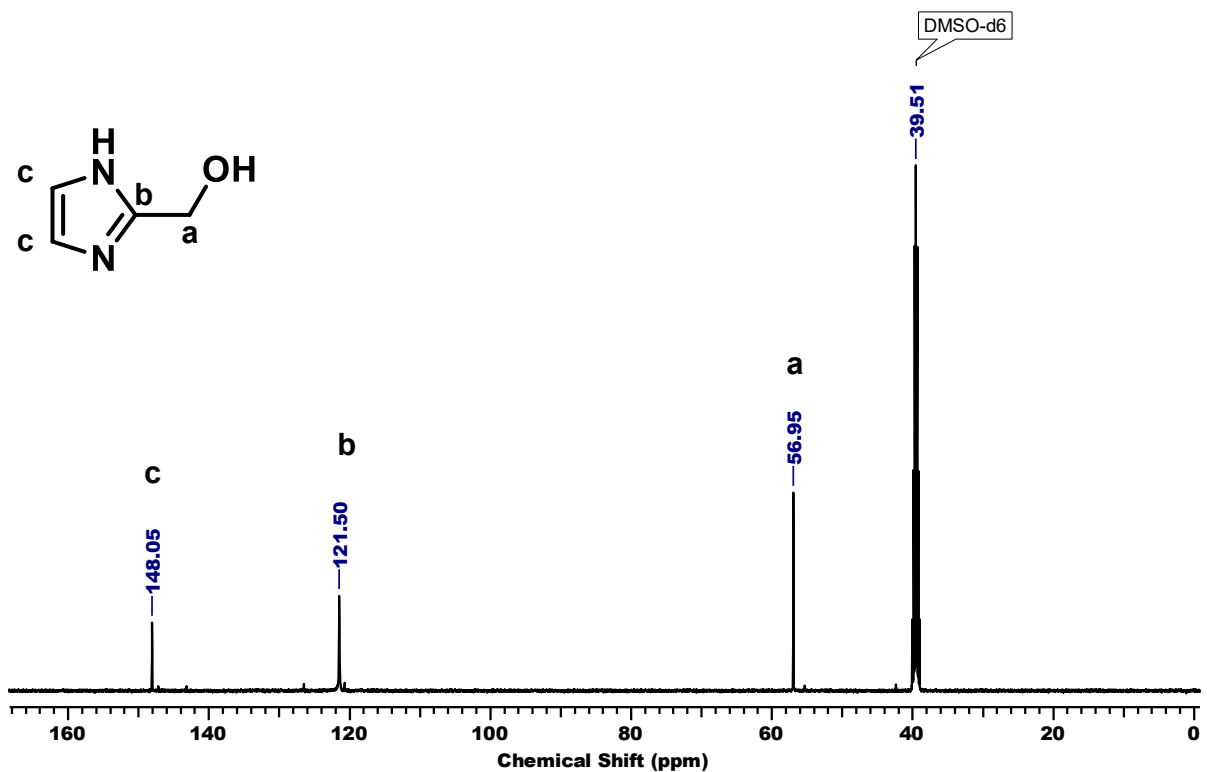
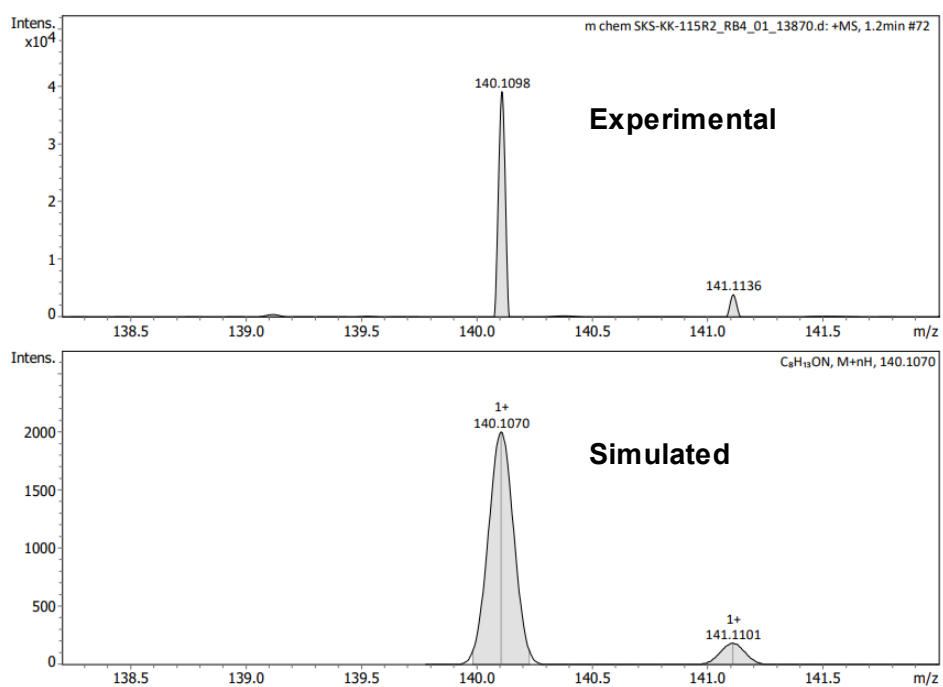
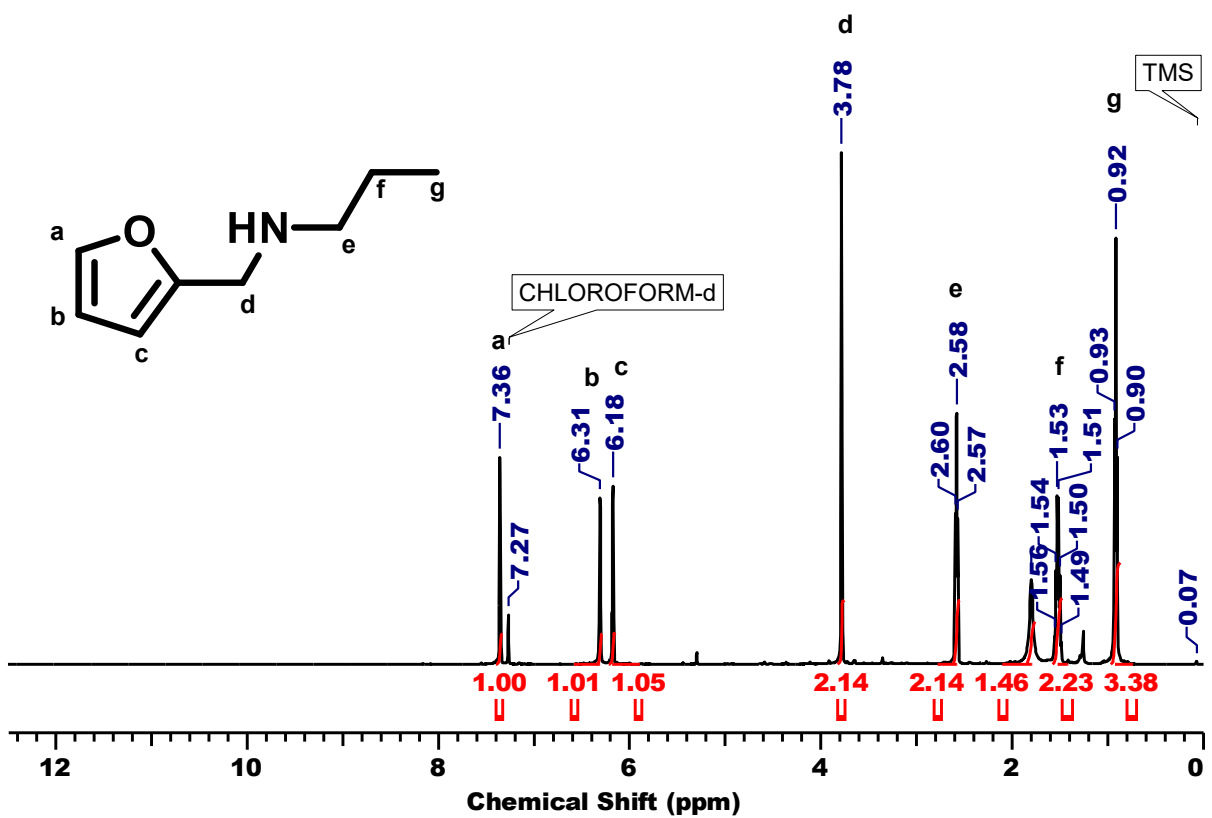


Fig. S25  $^{13}\text{C}$  NMR of L3



**Fig. S26** HR-MS spectrum of L4



**Fig. S27**  $^1H$  NMR of L4

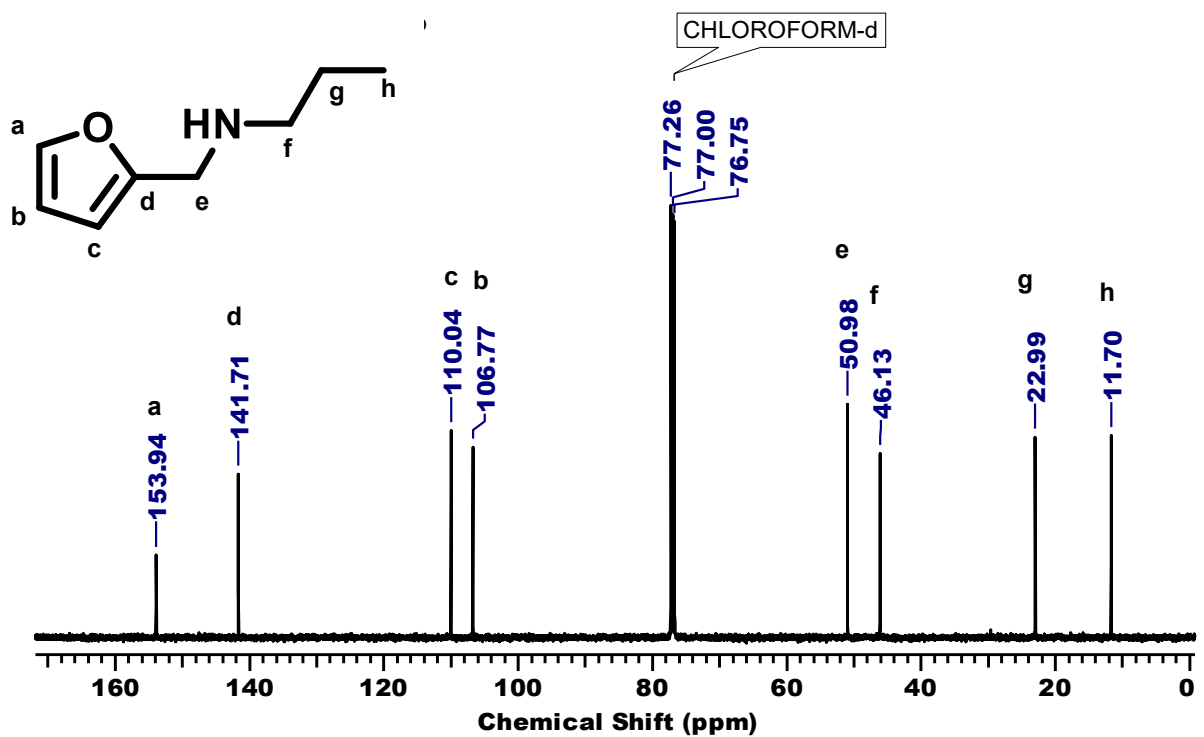


**Fig.S28**  $^{13}\text{C}$  NMR of L4

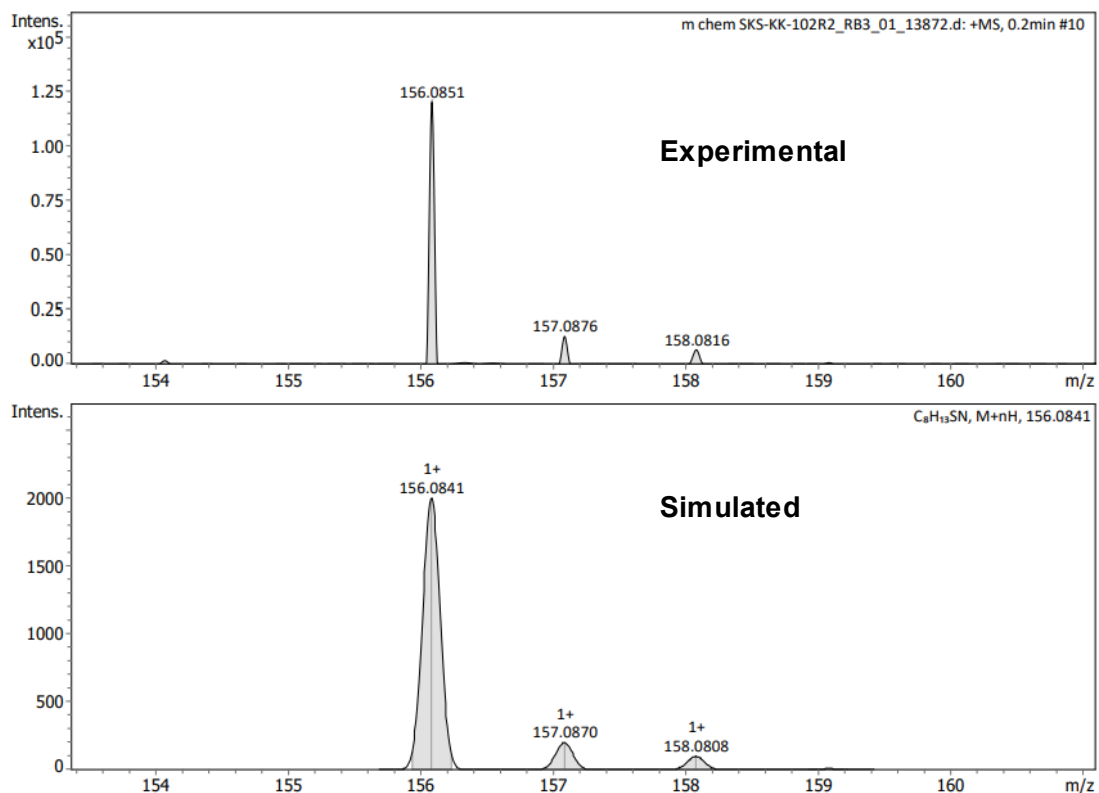


**Fig. S29** HR-MS spectrum of L5

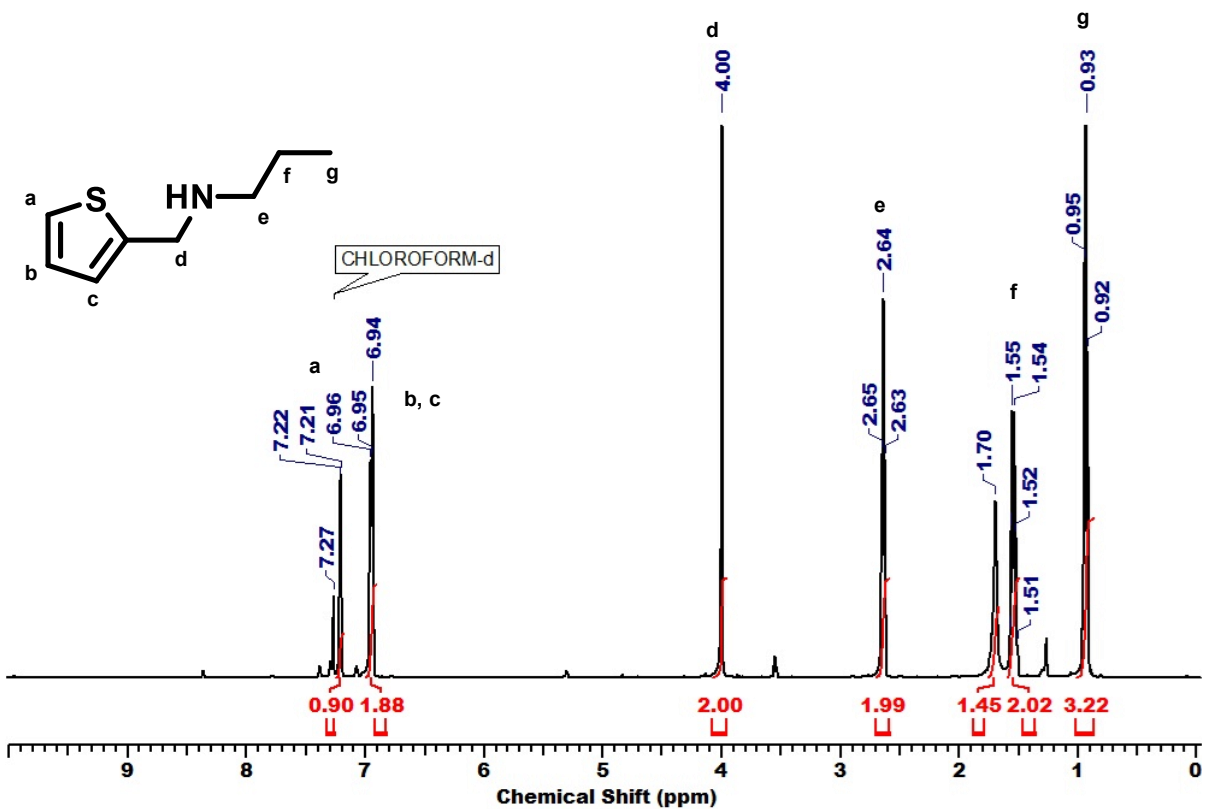


Fig. S30  $^1\text{H}$  NMR of L5

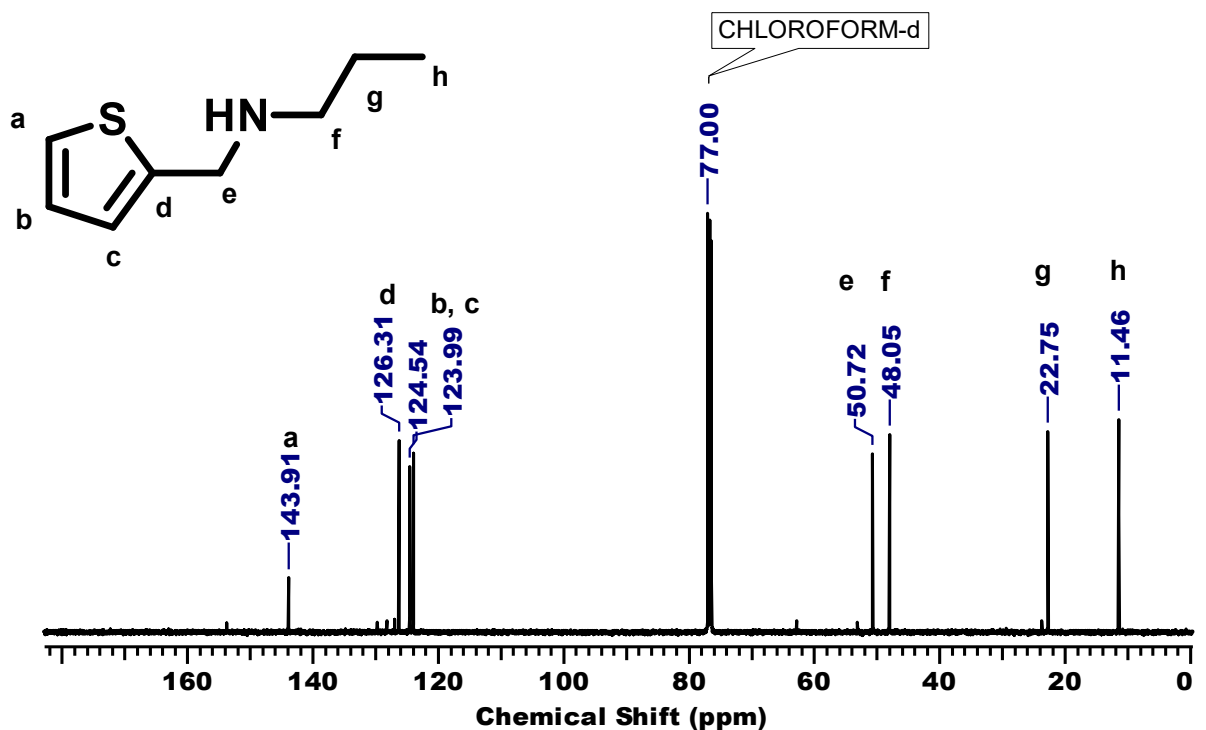
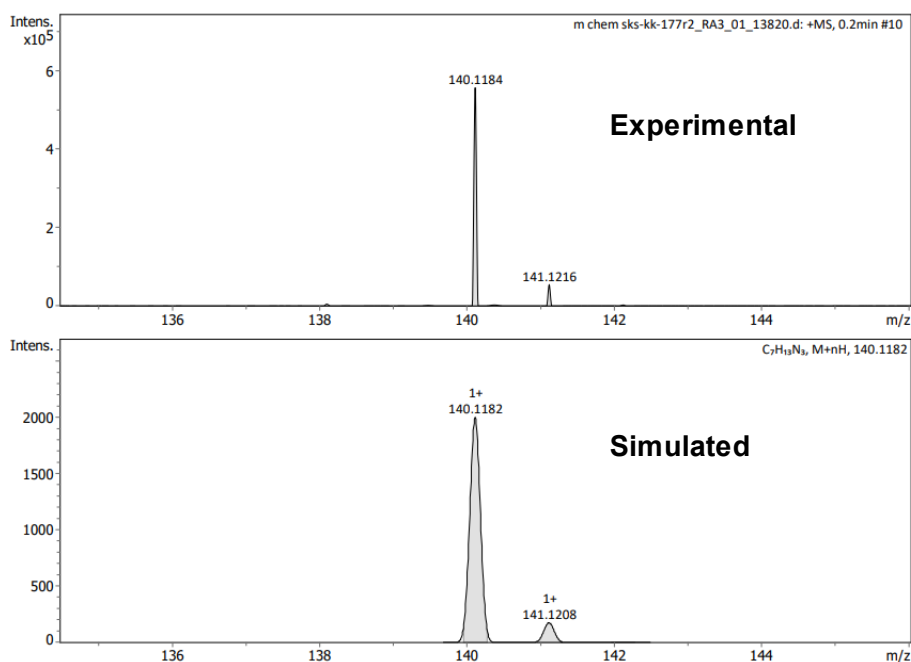
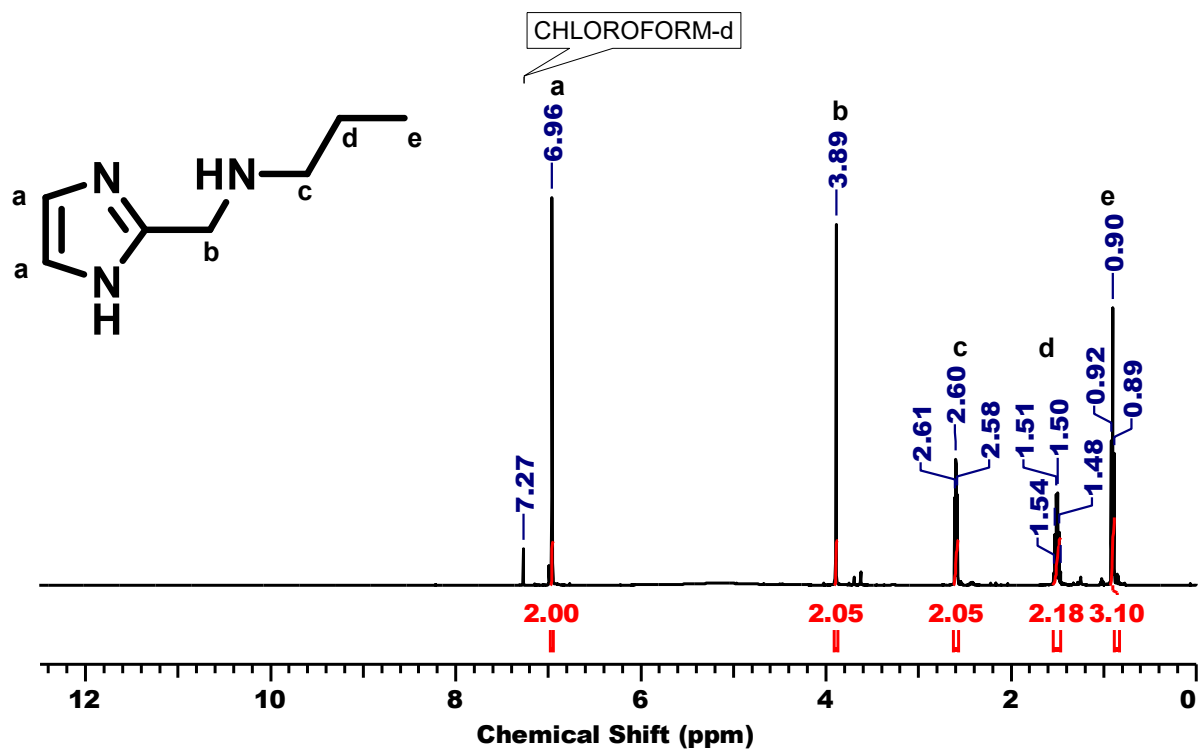


Fig. S31  $^{13}\text{C}$  NMR of L5



**Fig. S32** HR-MS spectrum of L6



**Fig. S33**  $^1\text{H}$  NMR of L6

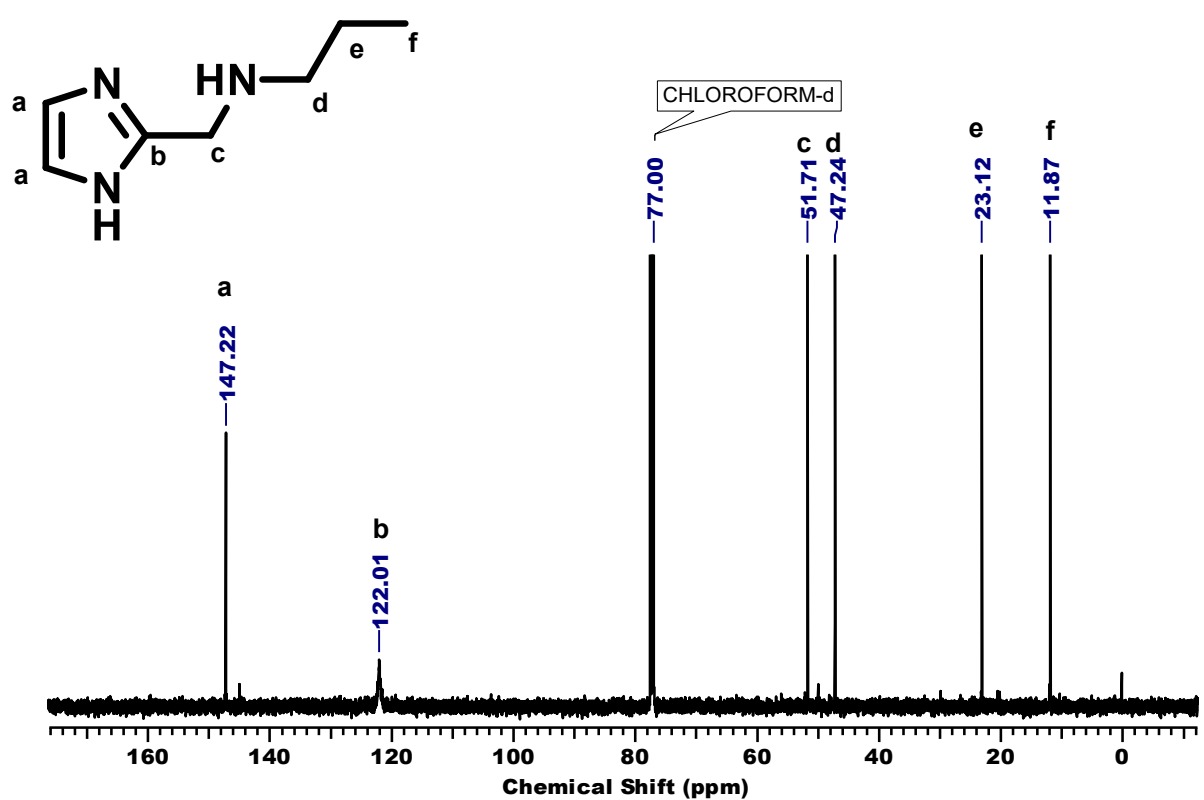


**Fig. S34**  $^{13}\text{C}$  NMR of L6

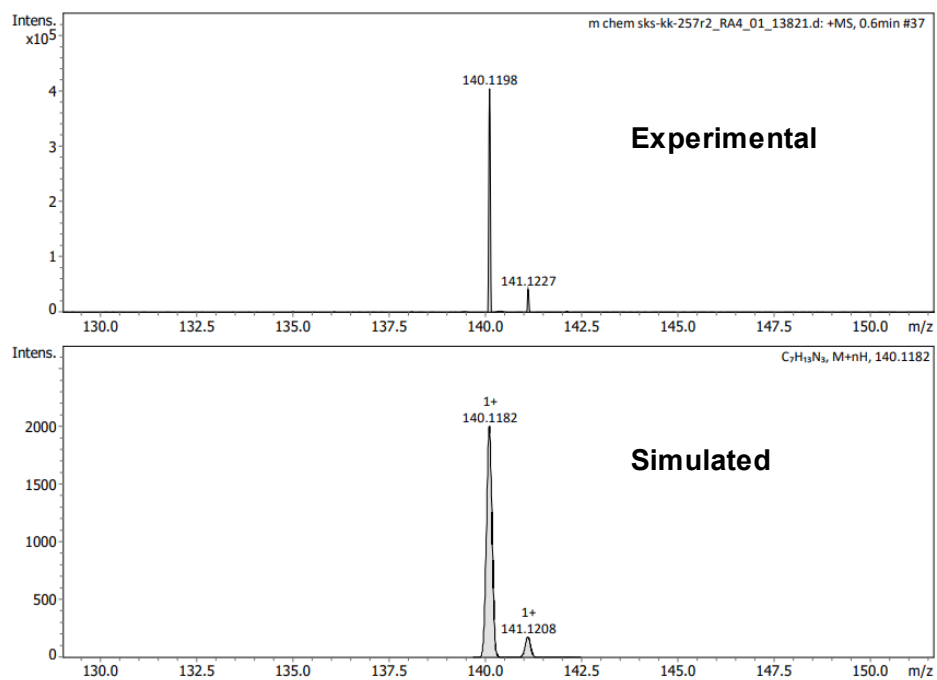


**Fig. S35** HR-MS spectrum of L7

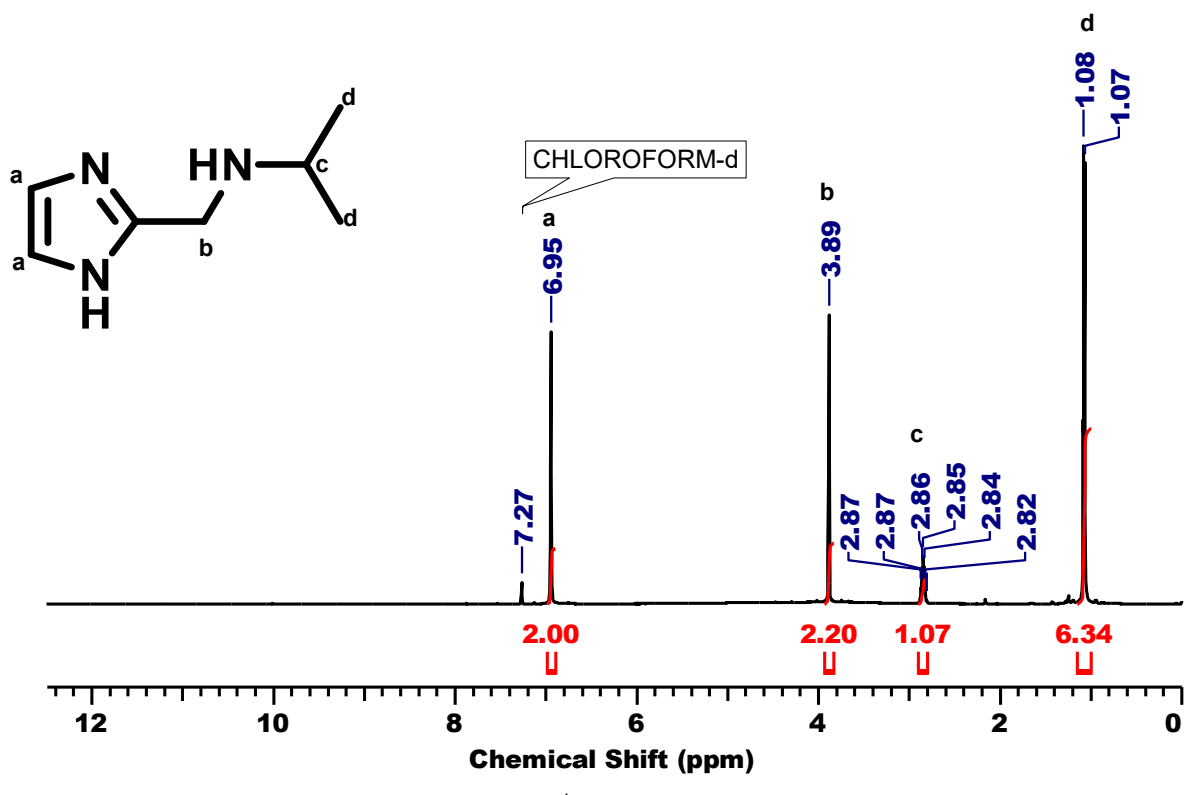


Fig.

S38 <sup>1</sup>H NMR of L7

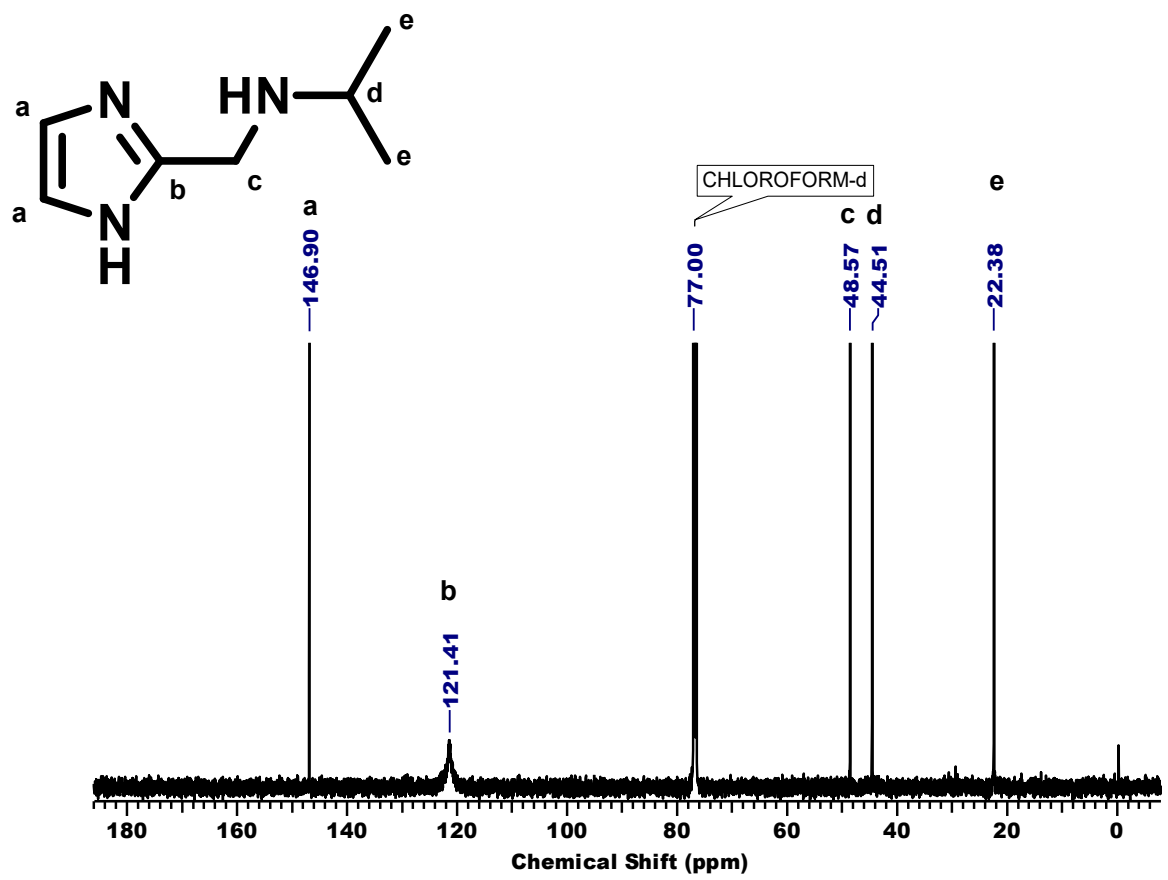
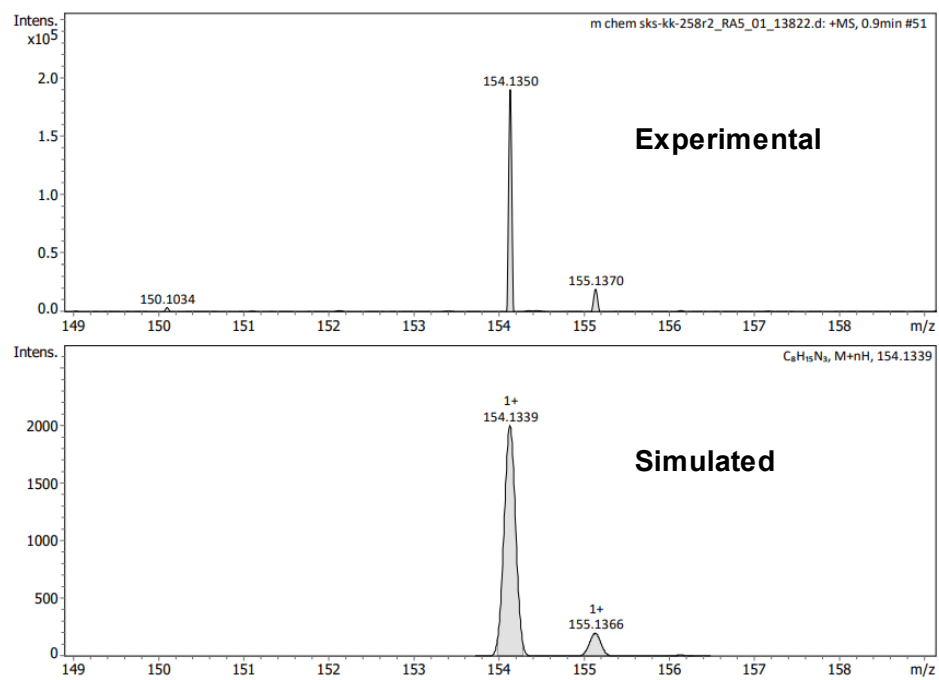
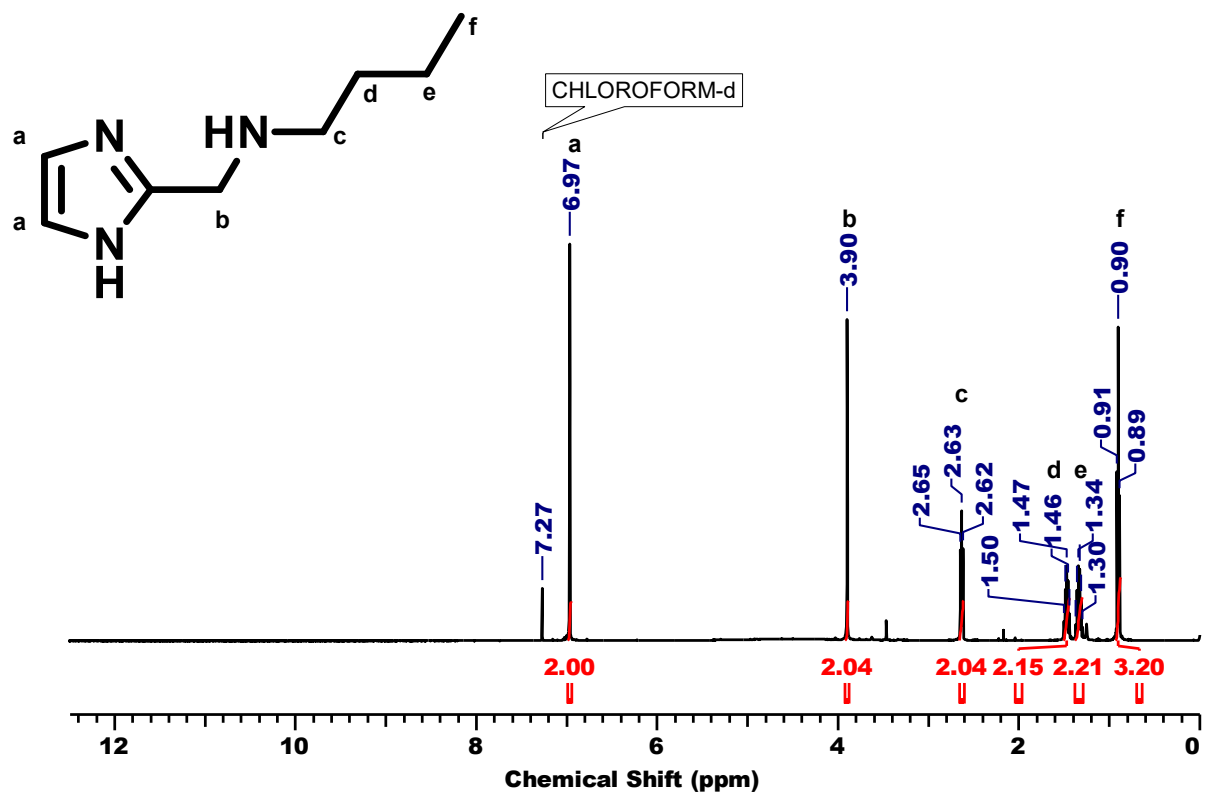


Fig. S37 <sup>13</sup>C NMR of L7



**Fig. S38** HR-MS spectrum of L8



**Fig. S39**  $^1\text{H}$  NMR of L8

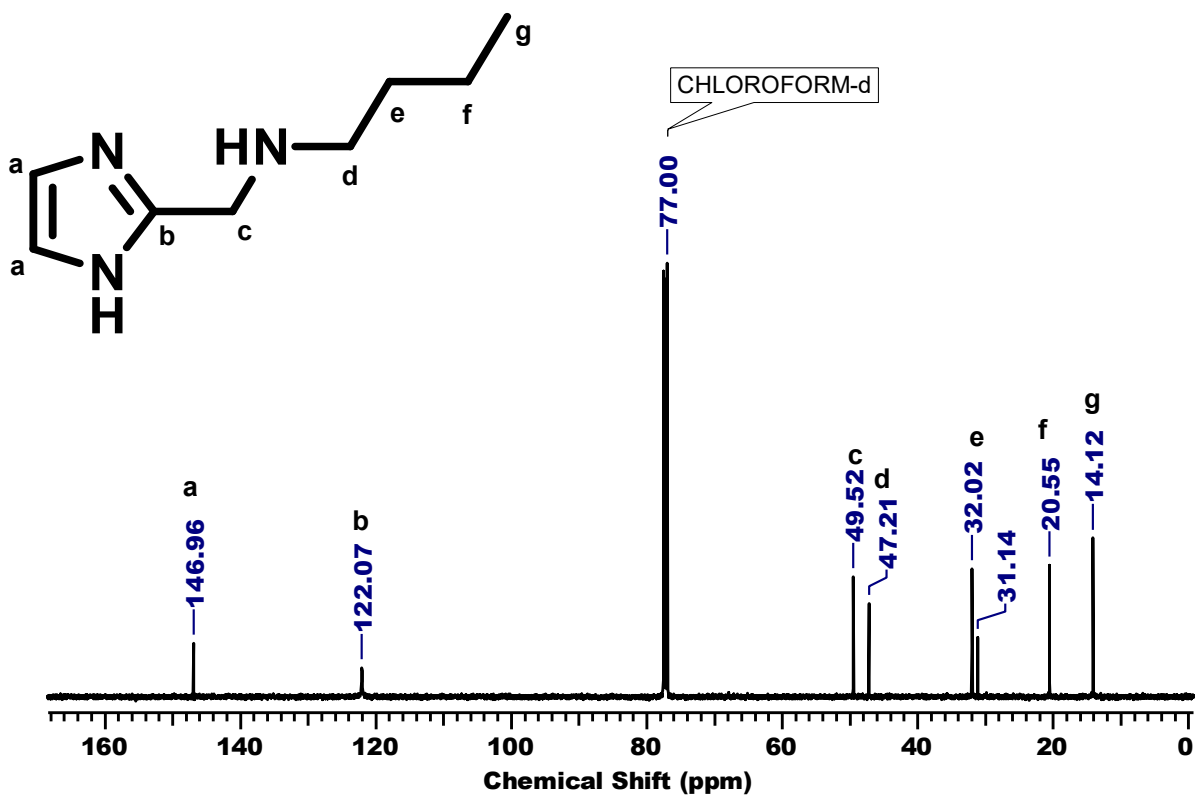


**Fig. S40**  $^{13}\text{C}$  NMR of L8

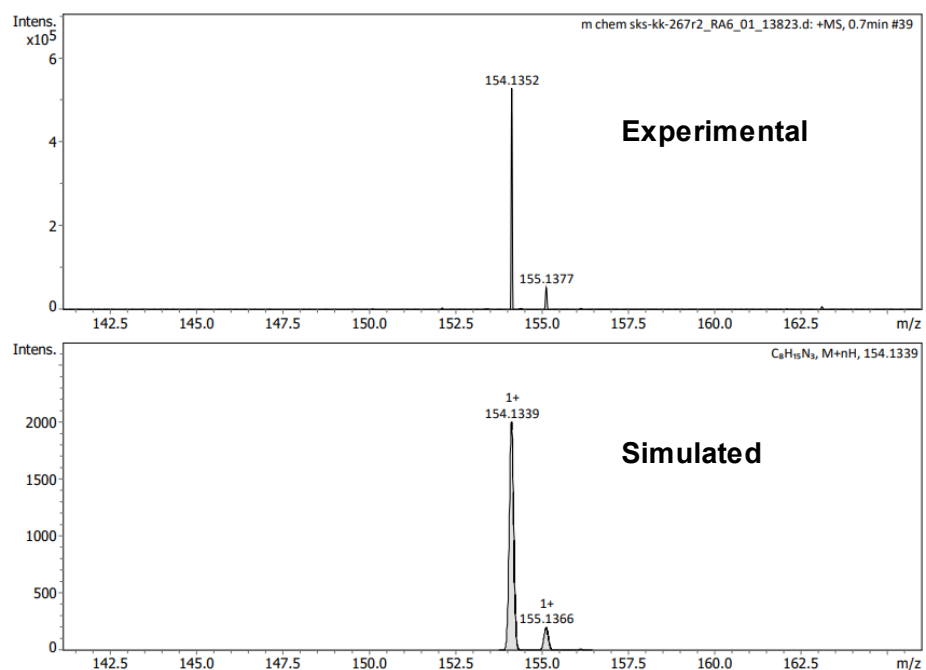


**Fig. S41** HR-MS spectrum of L9

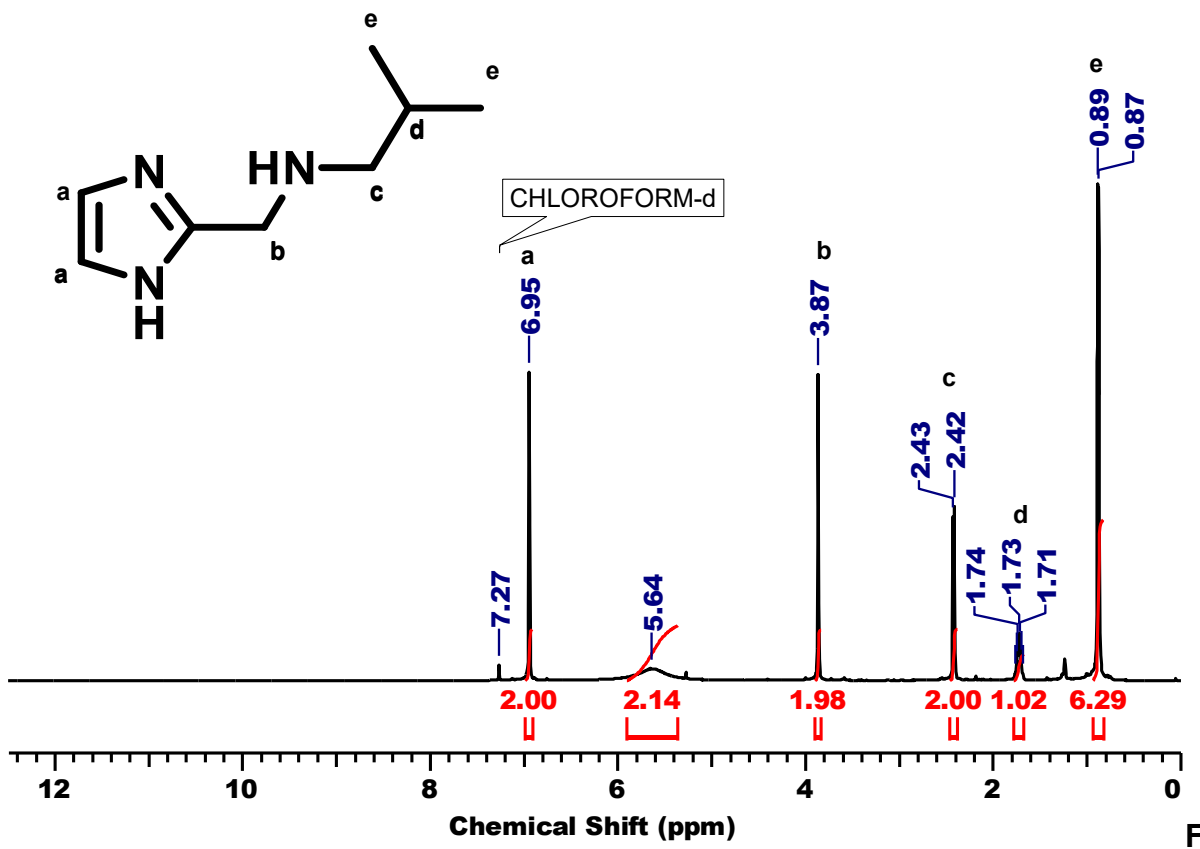


Fig.

S42  $^1\text{H}$  NMR of L9

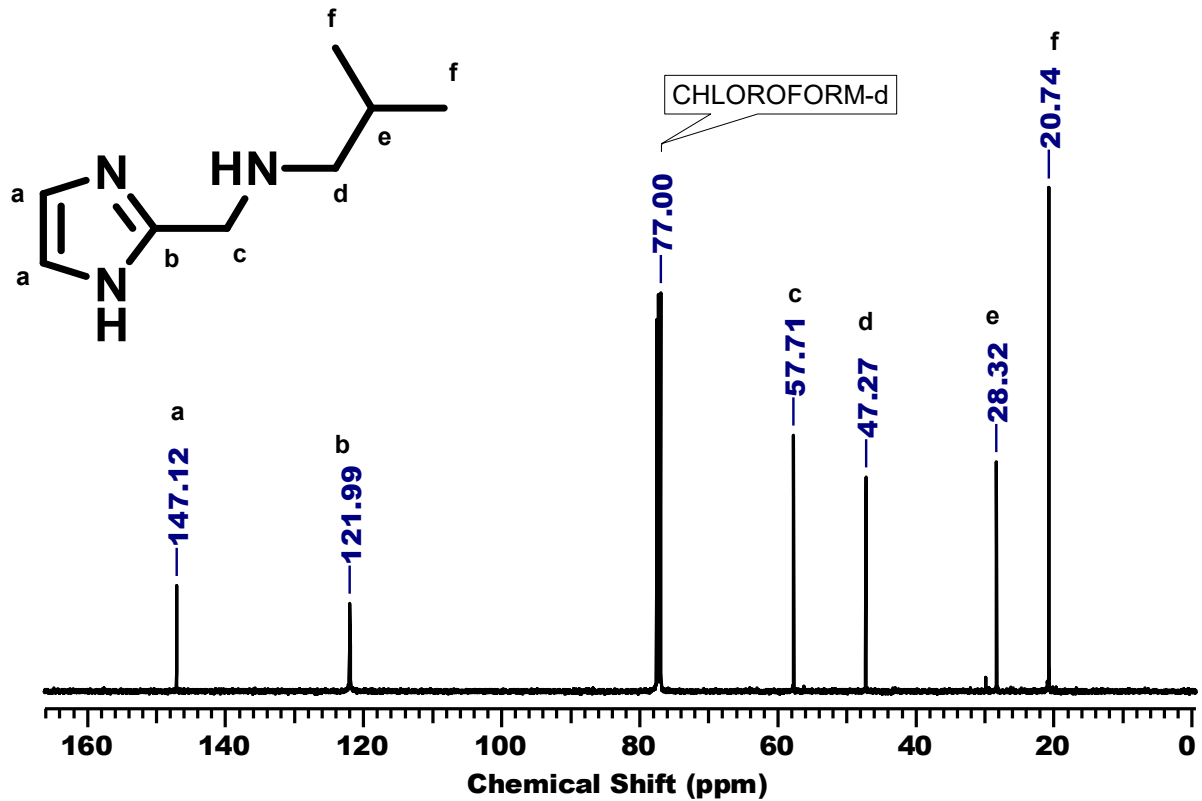
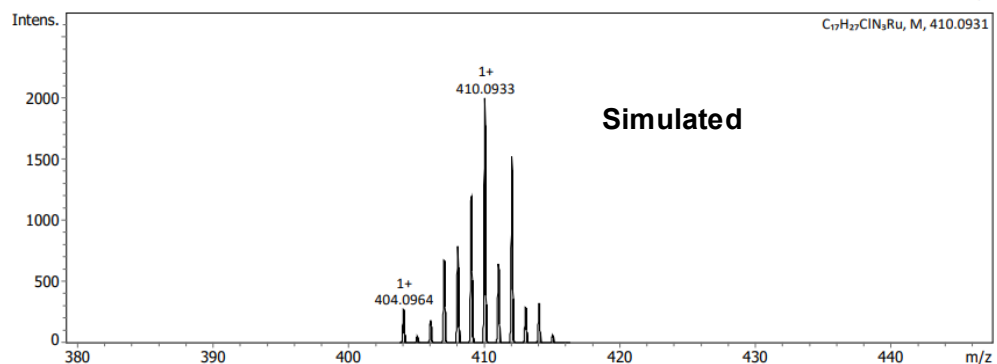
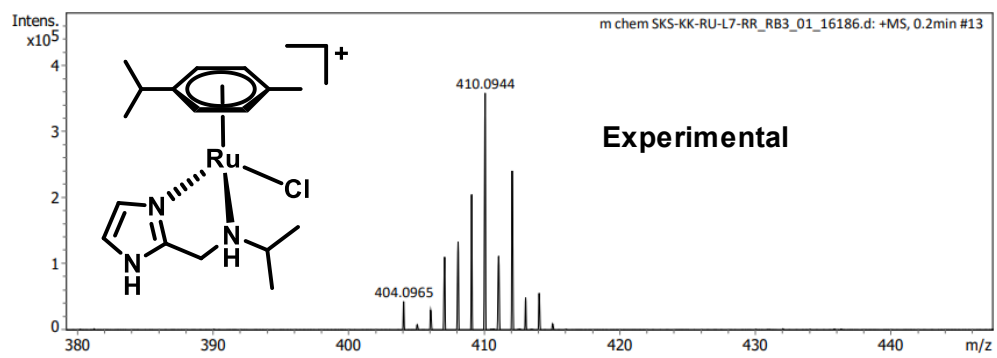
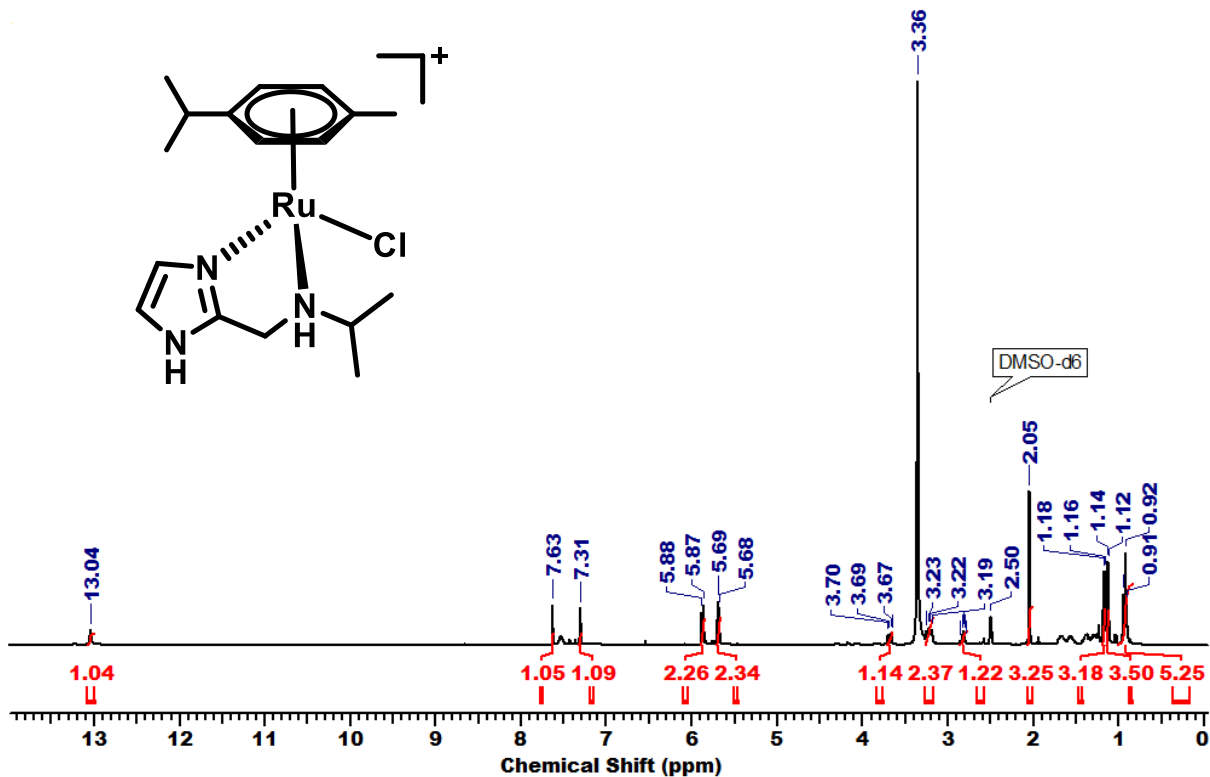


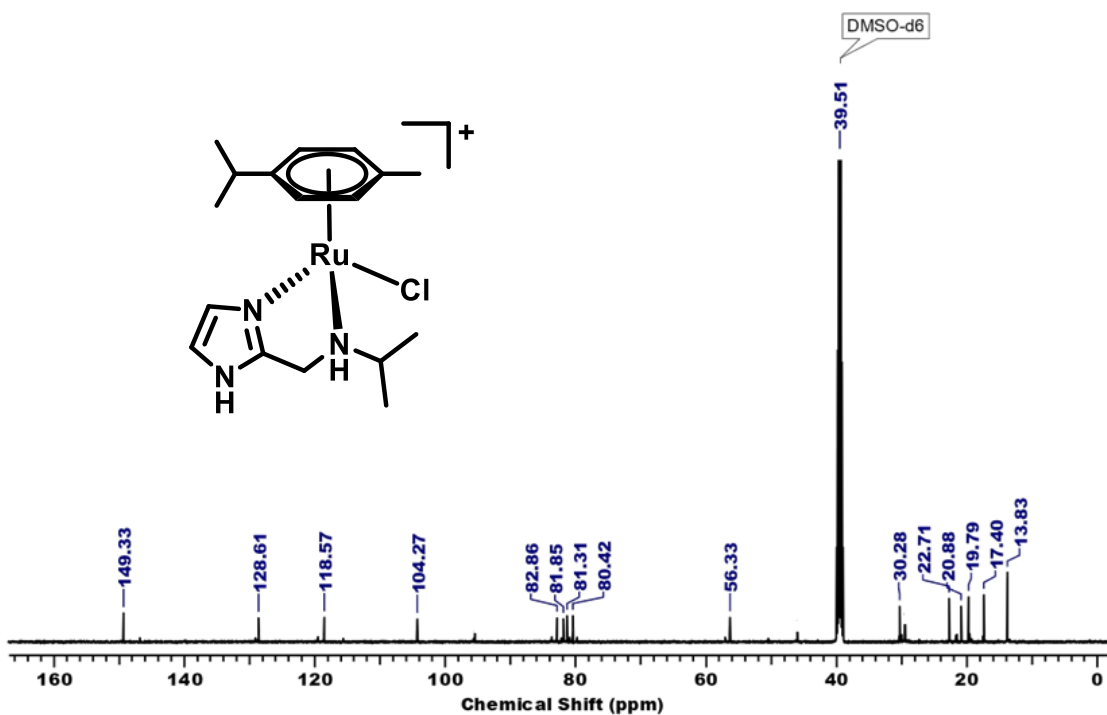
Fig. S43  $^{13}\text{C}$  NMR of L9



**Fig. S44** HR-MS spectrum of Ru/L7

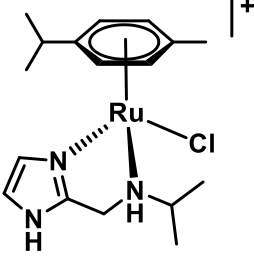
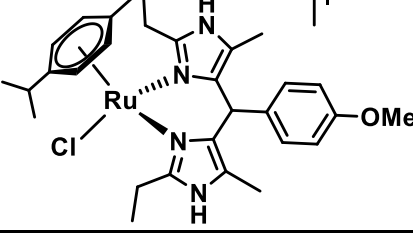
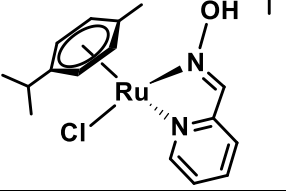
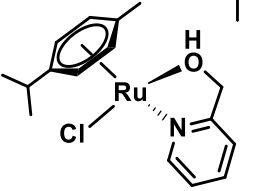
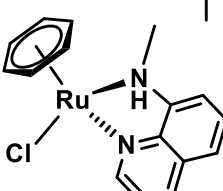


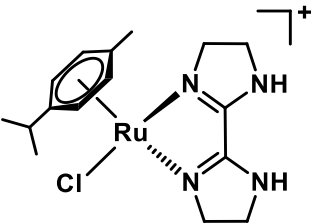
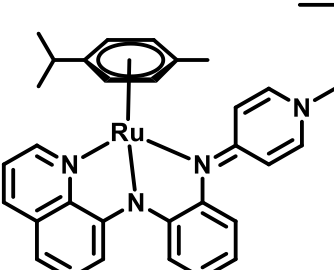
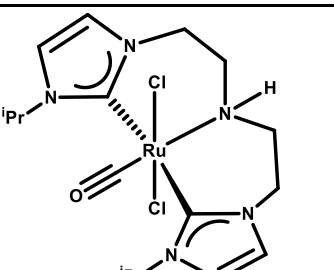
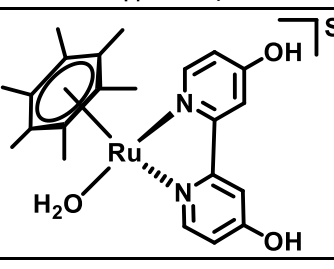
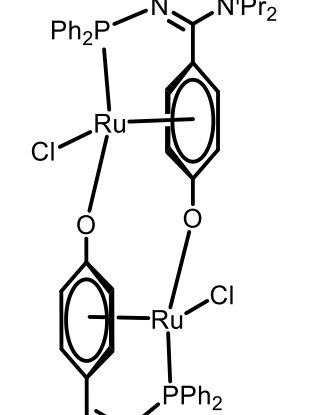
**Fig. S45**  $^1\text{H}$  NMR of Ru/L7



**Fig. S46** <sup>13</sup>C NMR of Ru/L7

**Table S11** Comparative catalytic activity of previous literature work and the current work for formic acid dehydrogenation.

Catalyst	Substrate	Solvent	T (°C)	t (h)	TON	TOF(h <sup>-1</sup> )	Ref.
	HCOOH/HCOONa	H <sub>2</sub> O	90	80	76,840	2000	This work
	HCOOH/HCOONa	H <sub>2</sub> O	90	0.33	8830	1545	S5
	HCOOH/HCOONa	H <sub>2</sub> O	90	1.56	500	296	S6
	HCOOH/HCOONa	H <sub>2</sub> O	90	0.25	6050	1548	S7
	HCOOH/HCOONa	H <sub>2</sub> O	90	0.25	2248	940	S8
[RuCl <sub>2</sub> (C <sub>10</sub> H <sub>14</sub> )] <sub>2</sub>	HCOOH	HexNMe <sub>2</sub>	40	3	30	10	S9
[RuCl <sub>2</sub> (PPh <sub>3</sub> ) <sub>3</sub> ]	HCOOH/NEt <sub>3</sub>	DMF	40	0.3	891	2688	S10
[RuCl <sub>2</sub> (C <sub>6</sub> H <sub>6</sub> )] <sub>2</sub> /DPPE	HCOOH	Me <sub>2</sub> NHex	80	NA	NA	47970	S11
[RuCl <sub>2</sub> (C <sub>6</sub> H <sub>6</sub> )] <sub>2</sub> /DPPE	HCOOH	DMOA	25	1080	>1000000	1000	S12
[(PNP <sup>3</sup> )Ru(H)Cl(CO)]	HCOOH / NHex <sub>3</sub>	DMF	90	3	706500	256000	S13
[(PNNNP <sup>2</sup> )RuH <sub>2</sub> (CO)]	HCOOH/NEt <sub>3</sub>	DMSO	90	150	1100000	7300	S14

	HCOOH/ HCOONa	H <sub>2</sub> O	90	29	350000	12000	S15
	HCOOH	DMSO	80	NA	2200	10000	S16
	HCOOH	1-ethyl-3-methylimidazolium diethylphosphate	100	3	2000	820	S17
	HCOOH	H <sub>2</sub> O	60	24	3700	94	S18
	HCOOH	DMSO	90	0.33	202	95	S19

HexNMe<sub>2</sub> = N,N-dimethylhexylamine; DMOA = dimethyloctylamine; DPPE = 1,2- Bis(diphenylphosphino)ethane.

## References

- S1 H. Kawanami, M. Iguchi and Y. Himeda, Ligand Design for Catalytic Dehydrogenation of Formic Acid to Produce High-pressure Hydrogen Gas under Base-free Conditions, *Inorg. Chem.*, 2020, **59**, 4191–4199.
- S2 W. H. Wang, M. Z. Ertem, S. Xu, N. Onishi, Y. Manaka, Y. Suna, H. Kambayashi, J. T. Muckerman, E. Fujita and Y. Himeda, Highly Robust Hydrogen Generation by Bioinspired Ir Complexes for Dehydrogenation of Formic Acid in Water: Experimental and Theoretical Mechanistic Investigations at Different pH, *ACS Catal.*, 2015, **5**, 5496–5504.
- S3 W.-H. Wang, S. Xu, Y. Manaka, Y. Suna, H. Kambayashi, J. T. Muckerman, E. Fujita and Y. Himeda, Formic Acid Dehydrogenation with Bioinspired Iridium Complexes: A Kinetic Isotope Effect Study and Mechanistic Insight, *ChemSusChem*, 2014, **7**, 1976–1983.
- S4 L. Guo, Z. Li, M. Cordier, R. Marchal, B. L. Guennic and C. Fischmeister, Noninnocent Ligands for Efficient Dehydrogenation of Aqueous and Neat Formic Acid under Base-Free Conditions, *ACS Catal.*, 2023, **13**, 13626–13637.
- S5 S. Patra, H. Deka and S. K. Singh, Bis-Imidazole Methane Ligated Ruthenium(II) Complexes: Synthesis, Characterization, and Catalytic Activity for Hydrogen Production from Formic Acid in Water, *Inorg. Chem.*, 2021, **60**, 14275–14285.
- S6 S. Kushwaha, J. Parthiban and S. K. Singh, Ruthenium-Catalyzed Formic Acid/Formate Dehydrogenation and Carbon Dioxide/(bi)carbonate Hydrogenation in Water, *Organometallics*, 2023, **42**, 3066–3076.
- S7 S. Patra and S. K. Singh, Hydrogen Production from Formic Acid and Formaldehyde over Ruthenium Catalysts in Water, *Inorg. Chem.*, 2020, **59**, 4234–4243.
- S8 S. Patra, M. K. Awasthi, R. K. Rai, H. Deka, S. M. Mobin and S. K. Singh, Dehydrogenation of Formic Acid Catalyzed by Water-Soluble Ruthenium Complexes: X-ray Crystal Structure of a Diruthenium Complex, *Eur. J. Inorg. Chem.*, 2019, **2019**, 1046–1053.
- S9 B. Loges, A. Boddien, H. Junge and M. Beller, Controlled Generation of Hydrogen from Formic Acid Amine Adducts at Room Temperature and Application in H<sub>2</sub>/O<sub>2</sub> Fuel Cells, *Angew. Chem. Int. Ed.*, 2008, **47**, 3962–3965.
- S10 C. Fellay, P. J. Dyson and G. Laurenczy, A Viable Hydrogen-Storage System Based On Selective Formic Acid Decomposition with a Ruthenium Catalyst, *Angew. Chem. Int. Ed.*, 2008, **47**, 3966–3968.

- S11 A. Boddien, C. Federsel, P. Sponholz, D. Mellmann, R. Jackstell, H. Junge, G. Laurenczy and M. Beller, Towards the development of a hydrogen battery, *Energy Environ. Sci.*, 2012, **5**, 8907–8911.
- S12 P. Sponholz, D. Mellmann, H. Junge and M. Beller, Towards a Practical Setup for Hydrogen Production from Formic Acid, *ChemSusChem*, 2013, **6**, 1172–1176.
- S13 G. A. Filonenko, R. Van Putten, E. N. Schulpen, E. J. Hensen and E. A. Pidko, Highly Efficient Reversible Hydrogenation of Carbon Dioxide to Formates Using a Ruthenium PNP-Pincer Catalyst, *ChemCatChem*, 2014, **6**, 1526–1530.
- S14 Y. Pan, C. L. Pan, Y. Zhang, H. Li, S. Min, X. Guo, B. Zheng, H. Chen, A. Anders, Z. Lai, J. Zheng and K.-W. Huang, Selective Hydrogen Generation from Formic Acid with Well-Defined Complexes of Ruthenium and Phosphorus–Nitrogen PN<sup>3</sup>-Pincer Ligand, *Chem. Asian J.*, 2016, **11**, 1357–1360.
- S15 C. Guan, D.-D. Zhang, Y. Pan, M. J. Ajitha, J. Hu, H. Li, C. Yao, M.-H. Huang, S. Min, J. Zheng, Y. Himeda, H. Kawanami and K. W. Huang, Dehydrogenation of Formic Acid Catalyzed by a Ruthenium Complex with an N,N'-Diimine Ligand, *Inorg. Chem.*, 2017, **56**, 438–445.
- S16 P. Knörr, N. Lentz and M. Albrecht, Efficient additive-free formic acid dehydrogenation with a NNN–ruthenium complex, *Catal. Sci. Technol.*, 2023, **13**, 5625–5631.
- S17 P. Aufricht, V. Nori, B. Rabell, L. Piccirilli, S. Koranchalil, R. W. Larsen, M. T. Nielsen and M. Nielsen, Formic acid dehydrogenation catalysed by a novel amino-di(N-heterocyclic carbene) based Ru-CNC pincer complex, *Chem. Commun.*, 2025, **61**, 3986–398.
- S18 Y. Himeda, S. Miyazawa and T. Hirose, Interconversion between Formic Acid and H<sub>2</sub>/CO<sub>2</sub> Using Rhodium and Ruthenium Catalysts for CO<sub>2</sub> Fixation and H<sub>2</sub> Storage, *ChemSusChem*, 2011, **4**, 487–493.
- S19 R. Verron, E. Puig, P. Sutra, A. Igau and C. Fischmeister, Base-Free Reversible Hydrogen Storage Using a Tethered π-Coordinated-Phenoxy Ruthenium-Dimer Precatalyst, *ACS Catal.*, 2023, **13**, 5787–5794.